Evolutionary Stability of Genetically Induced Trimethoprim Hypersensitivity in *Escherichia coli*

A Thesis

submitted to

Indian Institute of Science Education and Research Pune in partial fulfilment of the requirements for the MS Degree Programme

by

Manasvi Balachandran

Indian Institute of Science Education and Research Pune

Dr. Homi Bhabha Road,

Pashan, Pune 411008, INDIA.

Date: April, 2024

Under the guidance of

Supervisor: Dr Nishad Matange

Assistant Professor, Department of Biology, Indian Institute of Science Education and Research, Pune

From May 2023 to March 2024

INDIAN INSTITUTE OF SCIENCE EDUCATION AND RESEARCH PUNE

Certificate

This is to certify that this dissertation entitled **Evolutionary Stability of Genetically Induced Trimethoprim Hypersensitivity in *Escherichia coli*** towards the partial fulfilment of the MS degree programme at the Indian Institute of Science Education and Research, Pune represents study/work carried out by Manasvi Balachandran at Indian Institute of Science Education and Research under the supervision of Dr Nishad Matange, Assistant Professor, Department of Biology, during the academic year 2022-2023.

Dr Nishad Matange

Committee:

Dr Nishad Matange

Dr Sunish Radhakrishnan

This thesis is dedicated to my family and my friends.

i. Declaration

I hereby declare that the matter embodied in the report entitled **Evolutionary Stability of Genetically Induced Trimethoprim Hypersensitivity in *Escherichia coli*** are the results of the work carried out by me at the Department of Biology, Indian Institute of Science Education and Research, Pune, under the supervision of Dr Nishad Matange and the same has not been submitted elsewhere for any other degree. Wherever others contribute, every effort is made to indicate this clearly, with due reference to the literature and acknowledgement of collaborative research and discussions.

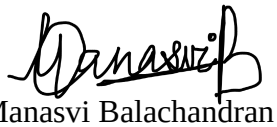

Manasvi Balachandran

20212003

Date: 15/03/24

Table of Contents

ii. # List of Tables

iii. List of Figures

iv. Abstract

Antibiotic resistance has compromised the ability to treat resistant infections and is a significant public health concern of the 21st century. These antibiotic resistant bacteria may possess natural intrinsic drug resistance such as due to a permeability barrier or acquire resistance by gaining mutations or new genetic material coding for antibiotic degrading enzymes. Several strategies such as bacteriophage therapy, antibiotic combination therapy and adjuvant therapy are currently being explored to reverse resistance. While the discovery of compounds that can reverse resistance is important, the identification of molecular targets that can modulate resistance is also equally crucial. Further, the evolutionary stabilities of the susceptibilities conferred by these targets is vital to ensure their introduction as therapeutics. In this study, we identified three potential targets of intrinsic resistance, *rfaG, lpxM* and *acrB,* that when deleted could modulate antibiotic susceptibilities and reverse trimethoprim resistance of *Escherichia coli.* At high trimethoprim concentrations, all 3 gene knockouts were jeopardised in their ability to recover from drug sensitivity. At low antibiotic concentrations however, they could evolve different extents of resistance by fixing different mutations that enabled them to adapt to trimethoprim. Significantly, the chemical inhibition of the AcrB target led to resistance evolution surpassing that of the evolved knockout, highlighting that they may overcome resistance through alternate mechanisms, and emphasising the need for monitoring and administration in antibiotic therapy.

v. Acknowledgments

I would like to thank Dr Nishad Matange for his guidance, support and mentorship throughout my thesis. His expertise and encouragement have been instrumental in shaping my academic journey. I would also like to thank all the past and present members of the Bugs and Drugs lab, specifically Rhea Vinchhi, Avani Joshi, Chetna Yelpure, Chinmaya Jena and Saillesh Chinnaraj for their mentorship and support. I would specifically like to express my appreciation to Ishaan Chaudhary for his invaluable contribution of data to this thesis. I would also like to express my gratitude to Dr. Sunish Radhakrishnan whose expertise and guidance provided important insights to my project.

I am deeply thankful to my parents, my sister, my grandmother, my cats, and all my friends (Aharna, Amisha, Anagha, Arya, Krittika, Lokesh, Manav, Mausami, Prarabdh, Ritvee, Rohan, Sakshi, Salima, Saleema, Sanhita, Shariyah, Siddhant, Srishti, Sultan, Vedant, Vidisha) for their love, encouragement and understanding.

Lastly, I would like to thank the Indian Institute of Science Education and Research Pune, for providing me with the resources and facilities required for my project. I would also like to express my gratitude to the housekeeping and administrative staff.

vi. Contributions

Contributor name	Contributor role
Manasvi Balachandran and Dr Nishad Matange	Conceptualization Ideas
Manasvi Balachandran and Dr Nishad Matange	Methodology
Manasvi Balachandran	Software
Manasvi Balachandran	Validation
Manasvi Balachandran	Formal analysis
Manasvi Balachandran, Ishaan Chaudhary and Dr Nishad Matange	Investigation
Dr Nishad Matange	Resources
Manasvi Balachandran and Dr Nishad Matange	Data Curation
Manasvi Balachandran	Writing - original draft preparation
Dr Nishad Matange and Manasvi Balachandran	Writing - review and editing
Manasvi Balachandran and Dr Nishad Matange	Visualization
Dr Nishad Matange	Supervision
Manasvi Balachandran and Dr Nishad Matange	Project administration
Dr Nishad Matange	Funding acquisition

1.Introduction

Antibiotics have transformed modern medicine, and have helped treat several bacterial infections and diseases. However, the rise in antibiotic resistance has compromised this ability to treat and prevent a growing number of bacterial infections. As a result, antibiotic resistance is one of the most significant public health concerns of the 21st century (Wise et al., 1998). Gram-negative bacteria makeup the most critical priority drug-resistant pathogens such as carbapenem-resistant *Acinetobacter baumannii* and *Pseudomonas aeruginosa* and extended-spectrum beta-lactamase (ESBL) producing *Enterobacteriaceae* (Willyard et al., 2017). A Review on Antimicrobial Resistance (AMR) published in 2016 by de Kraker described that AMR could be responsible for 10 million annual deaths by the year 2050 (de Kraker et al., 2016).

Murray in 2019, estimated that drug-resistant infections caused 4.95 million deaths worldwide, with 1.27 million directly attributed to antibiotic resistance across 88 pathogen-drug combinations (Murray et al., 2022). Despite efforts to develop new drugs to combat multidrug resistance (MDR), the situation remains highly complex. Only two classes of antibiotics, lipopeptides and pleuromutilins, have been introduced for clinical use against gram-negative bacteria over the past two decades (Hutchings et al., 2019). However, clinical isolates have developed resistance to these drugs, and their short-lived efficacy and low return on investment highlight the need to explore alternative strategies and therapeutics for treating AMR (Fitzgerald et al., 2019).

In order to devise strategies to overcome AMR, it is vital to understand how bacteria gain resistance. Bacteria may possess natural intrinsic resistance to a drug or acquire resistance by resistance-conferring genes or mutations (Martinez et al., 2014). Intrinsic resistance helps bacteria overcome naturally produced antimicrobial compounds and typically arises by modifying outer membrane permeability and efflux pump activity (Cox et al., 2013). For example, the MexAB-OprM efflux system confer beta-lactam and fluoroquinolone intrinsic resistance in *Pseudomonas aeruginosa*, an opportunistic gram-negative bacterium. *P. aeruginosa* also downregulates OprD2, a porin channel, which confers intrinsic imipenem resistance by altering the permeability of the outer membrane (Louis et al., 2006). On the other hand, acquired resistance is seen in clinically relevant bacterial populations that were initially vulnerable to antibiotics, and arises through vertical evolution or horizontal evolution (Cloeckaert et al., 2017, Chancey et al., 2012).

Molecular mechanisms of intrinsic and acquired resistance fall into four major categories - (i) limiting drug uptake; (ii) modifying the drug target; (iii) inactivating the drug; (iv) active drug efflux (Mahon et al., 2014) (Figure 1). Significantly, these mechanisms can occur simultaneously in bacteria, leading to an elevated level of resistance, and even giving rise to multi-drug resistance (Nikaido et al., 2009).

Figure 1.

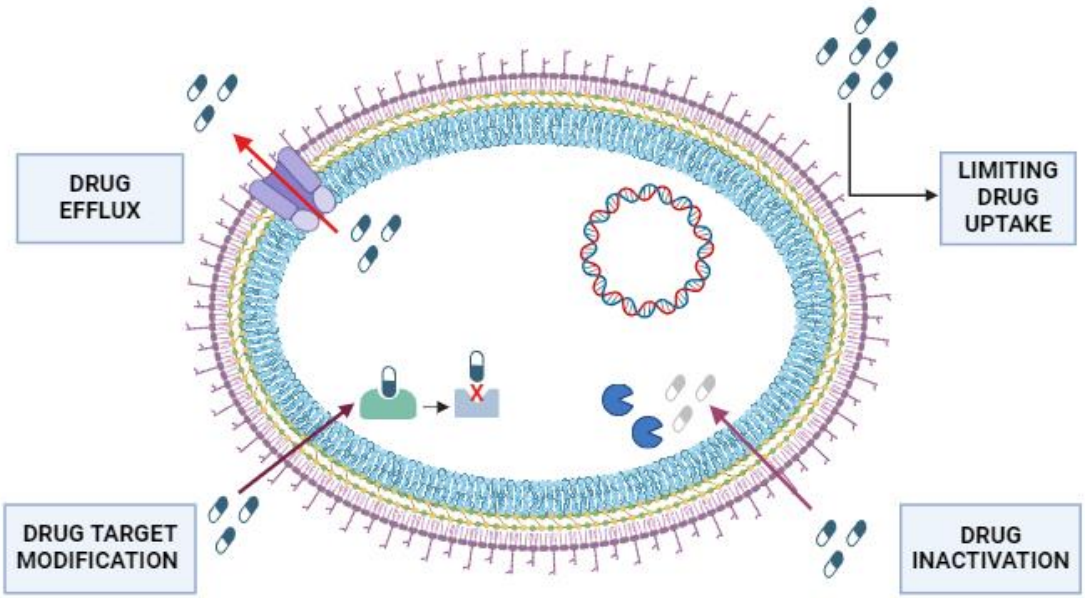

Figure 1: Schematic depicting general antimicrobial resistance mechanisms in gram negative bacteria. Created with BioRender.com

Hydrophilic antibiotics, such as tetracyclines and fluoroquinolones are especially affected by changes in the permeability of the outer membrane (Nikaido et al., 2003). Since these enter the cell through outer membrane porin channels, modification in the structure or expression of porin proteins leads to antibiotic resistance. For example, mutations in the *Escherichia coli* OmpF, OmpC and PhoE porin proteins are examples of permeability-related acquired resistance (Delcour et al., 2009). Efflux pumps transport several antibiotics out of the cell, and hence this mechanism of resistance usually affects a wide range of antibiotic classes, giving rise to multidrug resistance (MDR) (Nikaido et al., 2009). The AcrAB-TolC tripartite efflux pump in *E. coli* confers resistance to tetracyclines, chloramphenicol, novobiocin, some β-lactams, fluoroquinolones and fusidic acid when overexpressed (Hinchliffe et al., 2013).

While intrinsic and acquired resistance are influenced by cell permeability and drug efflux, other resistance mechanisms are limited to acquired resistance. One such mechanism of acquired resistance is drug target site modification that leads to a decreased affinity of the antibiotic to the drug target. For example, in *E. coli*, mutations occurring in the *folA* gene confer trimethoprim resistance by altering the drug target, dihydrofolate reductase (Watson et al., 2007). Beta-lactamase mediated enzymatic destruction of beta-lactam antibiotics is an example of acquiring resistance through enzymatic inactivation, another mechanism of acquired resistance. By cleaving the amide bond of the beta-lactam ring, beta-lactamases render the antibiotic ineffective. Genes that code for beta-lactamases are termed *bla* genes (Poole et al., 2004). For example, bla_{KPC} (*Klebsiella pneumoniae Carbapenemase)* is a class A beta-lactamase that degrades carbapenems (Nordmann et al., 2009).

The currently marketed antimicrobials represent a relatively small number of drug target types, and a substantial portion of these have had bacteria develop resistance against them. Therefore,

the identification of new cellular and molecular entities that can modulate resistance and have the potential to serve as drug targets is crucial (Sausville, 2012). Several studies have investigated alternative approaches to repurpose current treatment regimens and combat multidrug resistance, ranging from vaccinations, ethical farming, and improved diagnosis to the development of antimicrobial peptides, nanoparticles, and adjuvants (Payne et al., 2015). The strategies employed by these studies to address resistance ranges from the development of therapeutics designed to directly target the mechanism of acquired resistance, to designing therapeutics that impact general mechanisms implicated in intrinsic resistance.

1. Resensitization of resistant bacteria: recent trends in research

In order to understand trends in research concerning alternative treatment approaches for antibiotic-resistant bacteria and resensitize them to clinical antibiotic dosages, a comprehensive literature review was conducted. For this review, literature published between 2018 and 2023 on antibiotic resensitization were analysed for the strategies employed to overcome resistance. A total of 98 studies were analysed, which revealed that among the various strategies implemented, the most commonly explored strategy was found to be adjuvant therapy, followed by bacteriophage therapy, combination therapy, and gene silencing therapy (Figure 2). Other investigated strategies included collateral sensitivity, de novo strategies which comprised in-vitro gene knockout studies, human antibody-bacterial interaction studies and physical strategies that make use of pH, photodynamic light therapy and other physical stressors to achieve resensitization.

Figure 2.

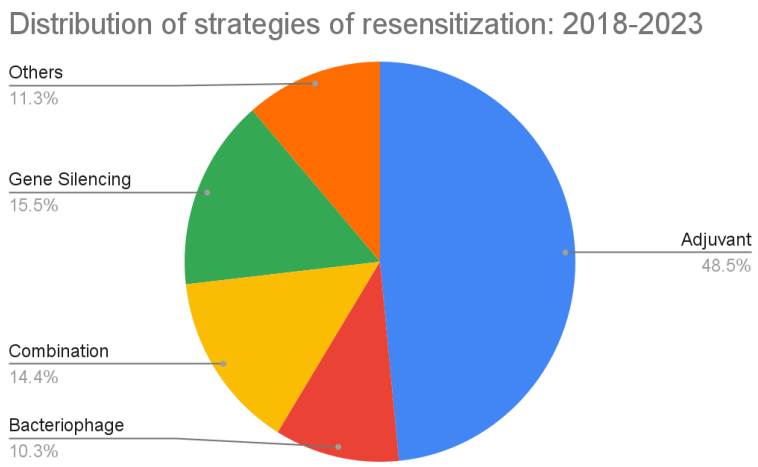

Figure 2: Distribution of alternative strategies employed between 2018 and 2023 to resensitize resistant bacteria, obtained from 98 search results.

Antibiotic adjuvant compounds, which are also referred to as "resistance breakers" or "antibiotic potentiators", are chemicals that exhibit minimal or negligible antibacterial

activity (Kalan et al., 2011). However, when administered concurrently with antibiotics, they can either (i) impede the primary bacterial resistance mechanisms or (ii) augment the antimicrobial efficacy of the antibiotic. The incorporation of adjuvants into antibiotic therapy is advantageous, as it eliminates the need for the laborious and costly identification of novel bacterial survival targets, and ensures the usage of the available range of antibiotics in the market (Wright et al., 2016). As of the present, numerous adjuvants have been extensively used in clinical practice, especially those compounds that inhibit the activity of beta-lactamases, which are responsible for conferring resistance to beta-lactam antibiotics. Some of the main types of adjuvants correctly being explored are described in the following sections:

2. Adjuvants for antibiotic modifying/inactivating enzymes

Adjuvants designed to reverse resistance mediated by antibiotic-inactivating enzymes are generally specific to a particular class of antibiotics. One of the most successful clinically-relevant adjuvants under this category are beta-lactamase inhibitors, which overcome resistance to beta-lactam antibiotics like penicillin. (Khanna et al., 2022). They behave like suicide inhibitors and permanently disable the enzyme via secondary chemical reactions in its active site. (Bush et al., 2016). Inhibitors of beta-lactamases are mostly prescribed for gram-negative bacterial infections, such as infections caused by *Enterobacteriaceae, Pseudomonas, Haemophilus* and *Neisseria*. Not only are these adjuvants effective against beta-lactamases, but also against extended-spectrum beta-lactamases. Therefore, they can reverse resistance to both β-lactams and cephalosporins, thus enhancing our capacity to overcome resistance (Buynak et al., 2004).

Some of the commonly used adjuvant/beta-lactam combinations include amoxicillin/clavulanic acid, sulbactam/ampicillin and ceftazidime/avibactam (Papp-Wallace et al., 2019). Modifications of existing beta-lactam inhibitors have also been shown to work against multi-drug resistant bacteria and resensitize them. For example, avibactam, a diazabicyclooctanone, was modified by Durand-Reville et al, 2017, to have small alkyl groups at the C3/C4 positions and a carboxamide in the C2 position. This modified adjuvant, ETX2514, was effective against classes A, C and D lactamases and was effective in restoring imipenem sensitivity to carbapenem resistant *Acinetobacter baumannii* and *Pseudomonas aeruginosa* (Figure 3). As seen in Figure 3, there is a clear decrease in the MICs for the carbapenem resistant strains upon the addition of ETX2514 to imipenem. This is far more effective than the combination of imipenem and relebactam against Carbapenem Resistant Enterobacteriaceae (CRE) strains, another clinically used beta lactamase inhibitor.

Figure 3.

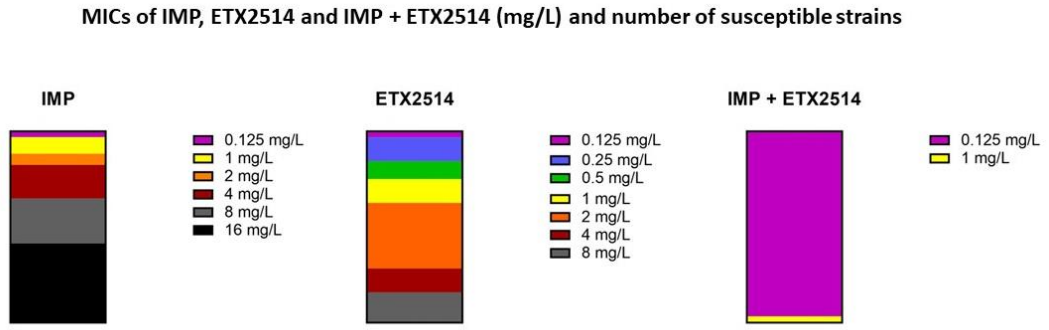

Figure 3: Schematic of antibacterial activity of ETX2514 and imipenem (IPM) alone or in combination against 32 CRE strains. Data replotted from Durand-Reville et al, 2017.

Two recently developed adjuvants in combination with imipenem-relebactam and meropenem-vaborbactam are effective against carbapenem-resistant Enterobacteriaceae and were approved for clinical use in 2019 (Zhanel et al, 2018). Relebactam, a β-lactamase inhibitor, is similar to avibactam, differing by the addition of a piperidine ring to the C2 group, whereas vaborbactam is a boronic acid based β-lactamase inhibitor. Metallo-β-lactamases use a Zn^{2+} activated water molecule to cleave the β-lactam ring, and several studies are exploring the displacement of the zinc ion to abrogate enzyme activity.

Djoko et al, 2018, tested the effect of copper ions on carbapenem-resistant clinical isolates of *E. coli* using a disk diffusion assay. While copper sulphate alone did not inhibit the growth of bacteria, when co-administered with ertapenem and meropenem, a dose-dependent zone of clearance was observed. Sun et al, 2020, also reported a similar finding when a combination of meropenem and auranofin, a gold-containing anti-rheumatoid drug, against MBL-positive *Enterobacteriaceae,* and observed a dose-dependent decrease in MICs, with increased potent bactericidal effect. They also showed that zinc ions were displaced by aurum ions using Equilibrium dialysis, and also observed that supplementation of zinc ions in the medium could not reverse the inhibition of MBLs. Auranofin is already an approved drug that exists in the market and has a well-recorded safety in humans, however, the effects and toxicity of the combination in vivo are yet to be tested (NCBI, 2023).

Unlike beta-lactamases, which inactivate the antibiotic by hydrolysing it, certain bacterial enzymes can cause antibiotic resistance by modifying vulnerable sites of antibiotics with different chemical groups, which prevents modified antibiotics from binding to their intended targets. For example, aminoglycosides have a core structure of amino sugars connected via glycosidic linkages to an aminocyclitol, which varies based on the specific subclass of aminoglycosides (Krause et al, 2016). These antibiotics are prone to modification due to the abundance of hydroxyl and amide groups on the surface of the aminocyclitol, and this enzymatic modification decreases the affinity of aminoglycosides to the 16S rRNA, their natural primary target.

There are three main classes of aminoglycoside modifying enzymes (AMEs); i) aminoglycoside acetyltransferases (AACs), ii) aminoglycoside nucleotidyltransferases (ANTs) and iii) aminoglycoside phosphotransferases (APHs). AACs are the most abundant AMEs and are found in gram-positive and gram-negative bacteria (Ramirez et al, 2010). Ahmed et al, 2020, identified four compounds, zinc pyrithione (ZnPT), vitamin E, vitamin D and vitamin K, via molecular docking, as potential inhibitors of AAC in clinical isolates of *E. coli* and *K. pneumoniae.* These compounds bound to the same active site as the substrate, and when combined with Amikacin or Gentamicin, gave rise to a significantly greater zone of inhibition in all three selected species. Enzyme activity assays also showed a reduced activity of AAC in *E. coli,* the highest decrease being observed for vitamin K (Ahmed et al., 2020). Research on adjuvants for aminoglycoside inactivating antibiotics, is however not very popular, and no progress has been made in this area in terms of clinical developments.

3. Adjuvants for enzymes modifying drug targets

Some enzymes that confer drug resistance are known to modify the drug target itself, therefore resulting in antibiotic resistance. For example, resistance to glycopeptides and colistin occurs due to the activity of enzymes that chemically modify elements of the bacterial cell envelope necessary for antibiotic binding. Colistin, a cyclic peptide, was once considered the last resort against MDR Gram-negative bacteria. However, due to its overuse, colistin resistance has emerged as a major concern (Liu et al., 2021). The global spread of the plasmid-mediated colistin-resistant gene *mcr* in Gram-negative bacteria has further exacerbated the problem. The *mcr* gene encodes a phosphoethanolamine (pEtN) transferase in *E. coli*, which catalyses the addition of pEtN to lipid A in LPS (Sun et al., 2018). This results in a significant decrease in the affinity between colistin and LPS, as the negative charge of lipid A is reduced. Therefore, there is an urgent need for novel and effective MCR inhibitors to combat bacterial infections.

Zhang in 2023 showed that the combined effect of an anti-diarrhoeal drug called loperamide, and colistin managed to resensitize *mcr*-1 positive *E. coli* and *K. pneumoniae* to colistin treatment. The MCR-1 protein interacted with loperamide with an equilibrium dissociation constant of 35.24 μM, as shown by standard molecular docking experiments. The same resensitization was also shown in mouse models, with no visible toxic side effects of the combination (Zhang et al., 2023).

Auranofin, which displayed potent bactericidal activity when combined with meropenem, could also restore colistin susceptibility in colistin-resistant *E. coli* by irreversibly displacing zinc ions from the MCR-1 protein equilibrium dialysis. The periplasmic domain of the MCR-1 protein binds to three equivalents of zinc ions, which are necessary for its function (Sun et al., 2020). The same phenotype was also observed in murine models infected with *E. coli* and *K. pneumoniae* containing different MCR variants.

4. Adjuvants for Efflux Pumps

Efflux pumps, present in all bacteria, serve as the primary mechanism for antibiotic resistance and multidrug resistance (MDR). Bacteria possess five different efflux pump superfamilies, which are categorised based on specific traits such as membrane topology, single or double membrane spans, energy sources, substrate specificity, primary sequence similarities, and multi-subunit complex stoichiometry (Webber and Piddock, 2003). These superfamilies include the small multidrug resistance family (SMR), ATP-binding cassette superfamily (ABC), resistance-nodulation-division superfamily (RND), multi-antimicrobial extrusion protein family (MATE), and major facilitator superfamily (MFS) (Figure 4).

Figure 4.

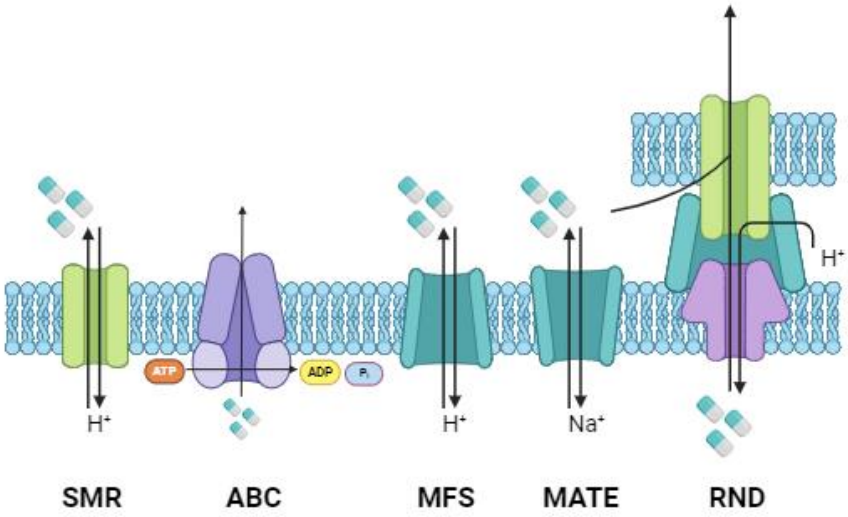

Figure 4: Schematic depicting five multidrug efflux pump families. Created with BioRender.com

Some bacterial efflux systems can efflux only a single class of antibiotics, such as TetA in *E. coli* which selectively excludes specific antibiotics like tetracycline. Others can pump out several classes of antibiotics and are designated as multidrug-resistant (MDR) efflux pumps (Poole et al., 2007). Most MDR efflux pumps are chromosomally encoded, such as the AcrAB-TolC complex in *E. coli* and MexAB-OprM in *P. aeruginosa*. However, some are plasmid encoded, such as QacA/B of *S. aureus*, or transposons, like MefA and MefB of *Streptococcus* spp., and provide horizontally-transferable modes of resistance.

Efflux pumps are promising and attractive targets for novel drugs, and several studies exploring efflux pump inhibitors (EPIs) as a valid strategy for combating antibiotic resistance are published (Marquez et al., 2005). For a compound to qualify as an EPI, it must satisfy the following criteria: (i) improve the effectiveness of antibiotics that are effluxed in strains that express functional pumps, (ii) be ineffective against strains that do not express efflux pumps, (iii) interact with a component of the efflux pump, (iv) not target any eukaryotic efflux pump and (v) possess ideal pharmacological features (Bhardwaj et

al., 2012). The search for EPIs is not a new one. Since the early 2000s, there have been experimental attempts to use EPIs to restore the effectiveness of antibiotics. The discovery of the first peptidomimetic EPI, phenylalanyl arginyl β-naphthylamide (PAβN), by Lomovskaya et al., 2001 was a significant breakthrough. When used in combination, PAβN enhanced the antibacterial properties of levofloxacin and erythromycin against multiple clinical *P. aeruginosa* isolates with an overexpressed MexAB-OprM efflux pump. However, the efficacy of EPIs has been limited so far, and none of them has been approved for commercial use.

EPIs can be classified into two general categories based on their mode of action - i) directly target and bind to a component of the efflux pump or ii) affect energy dissipation.

Efflux pumps rely on cellular energy, and separating the energy source from the pumping action could be a promising way to inhibit efflux. Inhibitors targeting the proton gradient or ATPase, which fuels the pumps, have been explored as potential efflux pump inhibitors (EPIs). This method does not require direct interaction with the efflux pump, and it could be advantageous since many pumps depend on the proton gradient, making it a universal and broad-spectrum approach to efflux inhibition. The efflux of tetracycline, an energy-dependent process, is linked to tetracycline resistance in numerous Gram-negative bacteria (Chopra et al., 2001). A study conducted by Anoushiravani et al., 2009, involving 112 isolates of *Helicobacter pylori*, which encompassed both tetracycline-susceptible and resistant isolates, demonstrated that over 70% of the isolates exhibited reduced MICs when exposed to a combination of tetracycline and carbonyl cyanide 3-chlorophenylhydrazone (CCCP). CCCP is an uncoupler of oxidative phosphorylation which disrupts the ionic gradient of bacterial membranes. Similarly, Sanchez et al., 2021, also showed that Imipenem-resistant *Acinetobacter baumannii* can be resensitized by a combination of CCCP and Imipenem, with MICs decreasing significantly by at least four dilutions. It has also been shown to resensitize several MDR *Enterobacteriaceae* to colistin, as shown by Sekyere et al., 2017, with MICs decreasing between 2 and 1024-fold for the selected isolates when a combination of CCCP and colistin were administered. Arsenate has also been shown to behave similarly to CCCP, as shown by Zeller et al., 1997 and inhibits the proton gradient, thereby conferring sensitivity to fluoroquinolones in *Streptococcus pneumoniae.* However, the in vivo activity and possible adverse side effects of CCCP has not been evaluated yet. Verapamil, a calcium channel blocker frequently prescribed for managing heart conditions, has also been identified as an inhibitor of ATP-dependent transporters and interferes with the generation of PMF (Gupta et al., 2014). Addition of Verapamil to bedaquiline resensitized bedaquiline-resistant *M. tuberculosis* strains.

Efflux pump inhibition can occur through another mechanism, which involves EPIs binding to functional efflux pumps. This binding reduces the pumps' abilities to interact with their substrates. The binding may be competitive or non-competitive. Nonetheless, bacteria can alter the target sites of these inhibitors, and render them ineffective.

One example of a target pump binding EPI is PAβN, as discussed previously. PAβN is a potentiator of levofloxacin and also erythromycin and chloramphenicol against *P. aeruginosa* expressing the MexAB-OprM efflux pump (Lomovskaya et al., 2001). The

effects of PAβN have also been studied on a wide variety of gram-negative bacteria that contain RND efflux pumps, including *Klebsiella pneumoniae* and *Acinetobacter baumannii.* This RND superfamily of efflux pumps contains multi-protein complexes that span the inner membrane (inner membrane protein), periplasmic space (periplasmic adapter protein), and outer membrane (outer membrane protein) of Gram-negative bacteria. Together, these proteins form a tripartite complex, and efflux occurs via a peristaltic mode through individual protomers of the RND component, because of the functional cycling of these protomers through loose, tight, and open states, which correspond directly to substrate access, binding, and extrusion (Nikaido et al., 2011).

Jamshidi et al., 2017, studied the interaction of PAβN with the AdeABC efflux pump in *Acinetobacter baumannii* computationally and found that there were strong hydrophobic interactions between Phe612 of AdeB and PAβN. Phe612 is situated at the tip of a hairpin-like loop, which divides the top of the channel between the proximal and distal binding pockets. The findings are in line with Takatsuka et al.'s observation, who, using molecular docking, saw that PAβN bound to the hydrophobic groove in the distal binding site of AcrB in *E. coli.* This prevents the pumps from moving through a series of conformational changes that are required for substrate efflux.

The NorA protein belonging to the MFS family of efflux pumps enables the efflux of fluoroquinolone antibiotics when overexpressed in *Staphylococcus aureus*. Fontaine et al., 2015, investigated the effects of a series of boronic derivatives against fluoroquinolone-susceptible and resistant *S. aureus.,* and found that inhibitors containing a boron atom for activity and a substituent in the para position with respect to the boronic moiety were the most effective in resensitizing *S. aureus* to ciprofloxacin. Thamilselvan et al., 2021, further showed that a derivative of boronic acid, 5-Nitro-2-(3-phenylpropoxy)pyridine (5-NPPP), showed binding within the transmembrane alpha-helices of NorA, via molecular docking, and also found that the combination of 5-NPPP and ciprofloxacin had a potentiating efficacy against clinical isolates of *S. aureus* and displayed increased bactericidal activity. 5-NPPP was also found to be non-toxic to mammalian cells. The next step would be to analyse its potency in in-vivo models.

Other modes of action for inhibiting drug efflux are being explored. These include the use of nanoparticle carriers, which release antibiotics at a local level, thereby overcoming the issue of secondary effects. Ding et al., 2018, synthesised silver-based antibiotic nanocarriers of various sizes conjugated with Ofloxacin and analysed the impact of these carriers on WT and Δ*ABM* (MexAB-OprM) in *P. aeruginosa.* They showed that the inhibitory effects of ofloxacin were highly dependent on its dosage, the sizes of the nanocarriers, and the expression of MexAB-OprM. Although nano-delivery has had limited success so far, technological advancements are expected to establish it as a promising strategy in combating antibiotic resistance.

5. Adjuvants for membrane permeability

The bacterial outer membrane is a formidable barrier to antibiotics. This is especially true for antibiotics that have cellular targets within the cell and not on the cell surface (Delcour et al., 2009). Gram-negative bacteria rely on the outer membrane (OM) to provide an additional layer of protection while still allowing for the exchange of necessary materials to sustain life. In most cases, the OM is an asymmetric bilayer composed of phospholipids and lipopolysaccharides (LPS). LPS is found exclusively on the outer leaflet and consists of three parts: lipid A, a phospholipid based on glucosamine, a short core oligosaccharide, and a distal polysaccharide called the O-antigen (Silhavy et al., 2010). It is not essential for the growth and survival of *Escherichia coli*; different strains may exhibit varying lengths of the core oligosaccharide and O-antigen.

Antibiotics utilize two distinct strategies to penetrate the bacterial wall, depending on their chemical properties (Chopra et al., 1988). Hydrophobic antibiotics, including macrolides and rifampicin, pass through the lipid bilayer utilizing passive transport mechanisms. On the other hand, hydrophilic molecules, such as β-lactams, and fluoroquinolones, employ active transport mechanisms to diffuse through the bacterial wall, by interacting with porins (Acosta-Gutierrez et al., 2018). The significance of the outer membrane barrier in antibiotic sensitivity is further supported by altered lipid or protein composition of the outer membrane of several drug-resistant pathogens. For instance, numerous reports indicate that antibiotic resistance has been acquired in a variety of organisms including *E. coli, P. aeruginosa, Neisseria gonorrhoeae, Enterobacter aerogenes, and Klebsiella pneumoniae* due to the loss or reduction of porins, or functional change of porins that reduce permeability (Ghai et al., 2018).

Previous literature has shown that targeting OM permeability is an efficient strategy for increasing antibiotic susceptibility. Renschler et al., 2022 showed that deletion of *surA*, a periplasmic chaperone involved in the biogenesis of outer-membrane proteins, leads to greater antibiotic susceptibility in multi-drug resistant *Acinetobacter baumannii* due to the loss of outer membrane integrity. Another commonly explored approach that has broad spectrum application is the development of adjuvants that work as membrane permeabilizers, therefore enhancing antibiotic uptake. Vaara et al., 1992 compiled and reported a list of compounds that work as outer membrane permeabilizers, which included lysine polymers, cationic peptides like lactoferrin, azurocidin, and chelators like EDTA and nitrilotriacetate, although information on increased bacterial susceptibility was not reported. Aboelenin et al in 2021, explored the effect of EDTA in modulating antibiotic susceptibility in multi-drug resistant (MDR) *P. aeruginosa*. Checkerboard analyses revealed that the addition of EDTA in combination with cefotaxime resulted in a significant decrease in MIC values. The effect of EDTA on the expression of porin genes confirmed a decreased expression of *mexA, mexB* and *oprM* genes in *P. aeruginosa* (Aboelenin et al., 2021).

Compounds with mild antimicrobial activity like silver and polymyxin derivatives have also been explored as adjuvants to enhance membrane permeability to antibiotics. Ramirez in 2013 used fluorescence intensity analysis to show that silver increased membrane

permeability in *E. coli* due to the disruption of disulphide bond formation and misfolded protein secretion. As a result, combination of silver and gentamicin increased the susceptibility of *E. coli* persister cells and eradicated biofilm formation (Ramirez et al., 2013). Along similar lines, Mu et al in 2022 explored the efficacy of a novel cationic polysaccharide conjugate Dextran-graft-poly(5-(1,2-dithiolan-3-yl)-N-(2-guanidinoethyl)pentanamide) (Dex-g-PSSn). Dex-g-PSSn in combination with rifampicin resensitized multidrug-resistant *Acinetobacter baumannii.* Dex-g-PSSn enhanced outer membrane permeability in a dose-dependent manner, and also disrupted the inner membrane (Figure 5). It also impacted efflux pump function and induced reactive oxygen species (ROS) build-up. It could effectively treat induced pneumonia when combined with rifampicin in mouse models with no obvious damage to lung tissue (Mu et al., 2022).

Figure 5.

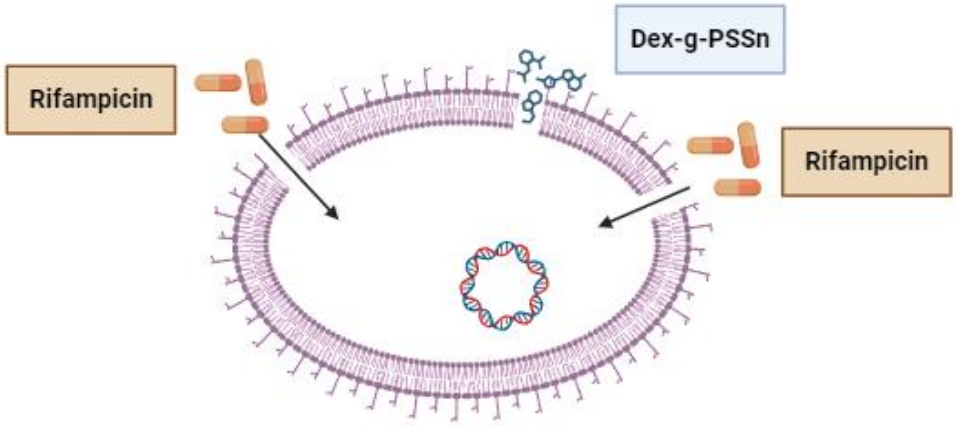

Figure 5: Schematic representing increase in outer membrane permeability and inner membrane disruption by Dex-g-PSSn. Adapted from Mu et al, 2022. Created with BioRender.com

Utilizing siderophores for antibiotic delivery across the gram-negative outer membrane is a "Trojan horse" strategy for combating antibiotic-resistant Gram-negative bacteria (Schalk et al, 2018). Siderophores are secondary metabolites that bacteria secrete to scavenge iron from the environment and transport it into the bacterial cell through specific outer membrane receptors and membrane bound TonB-ExbB-ExbD complex (Raines et al., 2015). Cefiderocol is a first-in-class compound clinically approved siderophore adjuvant that utilizes a synthetic siderophore mimic and demonstrates efficacy against a variety of carbapenem-resistant Gram-negative pathogens (Yamano et al., 2019). Halasohoris et al, 2021 analysed the effects of GT-1 (LCB10-0200), a novel siderophore antibiotic conjugate (SAC) on an array of multi-drug resistant and biothreat pathogens, including *E. coli, P. aeruginosa, A. baumannii*, and *K. pneumoniae.* The addition of GT-1 significantly improved MICs to beta-lactams compared to single treatment. Membrane permeabilizers are therefore excellent adjuvants that can help reverse both intrinsic and acquired resistance and have the potential to become indispensable in treating drug-resistant bacteria.

6. Scope of the present study

While the above-mentioned strategies are effective in resensitizing and eliminating drug-resistant bacteria in in-vitro and less frequently in-vivo, very few studies that document the evolution of resistance to these resistance-breakers have been carried out. This is worrisome because the development of resistance to resistance-breakers is not a new concept. Studies from as early as 1992 (Vedel et al., 1992) have reported the evolution of resistance against beta-lactamase inhibitors in almost all clinically relevant pathogens due to the exacerbated use of antibiotic-adjuvant combinations. Furthermore, the limited body of research examining the evolutionary dynamics of resistance to therapeutic agents predominantly focuses on combating acquired antibiotic resistance. There exists a notable gap in the exploration of intrinsic resistance as a viable target and an insufficient investigation into its evolutionary stability. Additionally, the proposed modulators of intrinsic resistance in the above studies such as efflux pump inhibitors suffer from solubility, toxicity and permeability problems, making them unsuitable for clinical use.

In this study, we took a genetic route to identify potential targets that could modulate intrinsic mechanisms of resistance in *Escherichia coli*. Using trimethoprim, an antifolate antibiotic, a genetic screen was performed in a laboratory strain of *Escherichia coli* to identify genes involved in cell wall processes, metabolism and transport that modulate intrinsic antibiotic susceptibility.

7. Objectives of the study

i) Identify genetic modulators of intrinsic resistance that can confer hypersensitivity to trimethoprim in different strains of *Escherichia coli*, and reverse trimethoprim resistance.
ii) Study their ability to confer sensitivity to other antibiotics.
iii) Determine and compare the evolutionary stabilities of hypersensitive phenotypes in high-drug and low-drug concentrations of trimethoprim, and track the genomic changes associated with overcoming trimethoprim hyper susceptibility.
iv) Compare the sensitivities conferred by genetic and chemical modifiers of intrinsic resistance and document the differential capabilities of genetic and chemical modifiers of resistance to evolve trimethoprim resistance.

2. Materials and Methods

2.1 Materials

a) **Glassware, plasticware and related materials:** All glassware utilized in the study was sourced from Borosil Glass Works Ltd (India) and Schott Duran (Germany). Plasticware items were obtained from Tarsons Products Pvt. Ltd. (India) and HiMedia (India). Sterile 96-well plates were procured from HiMedia (India). Consumables like 0.2mm filters, syringes, and metal wire-loops were procured from HiMedia (India), and parafilm, 1.5 ml micro-centrifuge tubes (MCTs), pipette tips, and aluminum foil, were sourced from Tarsons Products Pvt. Ltd. (India), Corning Life Sciences (India), and FoilPlus (India), respectively. Pipette sets were obtained from Eppendorf (India).

b) Instruments

Table 1: List of instruments used in the study.

INSTRUMENT	USAGE	SYSTEM DETAILS
Refrigerators (-80°C, -20°C, 4°C)	Storage of glycerol stocks, antibiotic stocks, primers and other chemicals	Panasonic
Incubator (with shaking facility)	Incubation of bacterial cells at 37°C	New Brunswick Innova 42
Laminar Air Flow Unit	All Microbiology work (Inoculation, Plating, Broth Dilution Assay, Serial Dilution Spot Assay, Adaptive Laboratory Evolution, Checkerboard Assay)	MicroFilt India, Krew Instruments
Gene Box	Imaging of agarose gel, Imaging of plates	GeneSys
96 Well Plate Reader	Measurement of optical density (OD) for Broth Dilution Assays, performed in 96 well plates	Ensight by Revvity
Thermal Cycler	Polymerase chain reactions	Eppendorf Master Cycler x 50s, Eppendorf vapo.protect
Mini-centrifuge	Genomic DNA isolation and purification, spinning down bacterial cultures	Minispin by Eppendorf
Spectrophotometer	Verification of quantitiy and purity of genomic DNA	Thermo-scientific NANODROP 2000c
Gel Power supply	Submerged horizontal gel electrophoresis	Bio-Rad Powerpac Basic

c) **Chemicals**

Table 2: List of chemicals used in the study

HiMedia	Sigma LifeSciences	Invitrogen	SRL	MPBio
LB Powder	CH_3CH_2OH	Glycerol	$Na_3C_6H_5O_7$	Sodium Dodecyl Sulphate
LA Powder	$CaCl_2$			
Ethidium Bromide	DMSO			
CH_3COONa	Phenol Chloroform Isoamyl alcohol (PCI)			
Agarose Special, low EEO				
$CHCl_3$				

d) Fine chemicals

Table 3: List of fine chemicals used in the study

Fine Chemical	Source	Catalogue number
ProteinaseK	Sigma	Cat#1073930010
RNase A	Sigma	Cat#10109142001
PrimeSTAR Max	Takara	Cat#R045
ReadyMix Taq PCR	Sigma	Cat# 1003397971

e) Antibiotics/antipsychotic

Table 4: List of antibiotics/antipsychotic used in the study

Antibiotic/antipsychotic	Solvent	Source	Catalogue number
Trimethoprim	(100%) DMSO	Sigma	Cat#T7883
Chloramphenicol	100%) C_2H_5OH	HiMedia	Cat#CMS218
Kanamycin	Autoclaved MilliQ filtered water	SRL	Cat#4230027
Chlorpromazine	Autoclaved MilliQ filtered water	Sigma	Cat#1003484716

f) **DNA ladders/markers**

Table 5: List of DNA ladders/markers used in the study

Ladder/marker	Range	Source
Invitrogen 1kb+ DNA ladder	100bp-15kb	Invitrogen
Takara	100bp-1500bp	DSS Takara Biosciences
Gel loading dye purple	NA	New England Biolabs

g) **List of PCR primers**

Table 6: List of primers used in the study

Primer name	Primer Sequence (5' – 3')	Purpose	Source
rfaG_upstream_fw	CAGCTGACAGGAATGCACAATTATG	Forward primer for confirmation of *rfaG* knockout by PCR	Sigma
acrB_upstream_fw	CTTAAACAGGAGCCGTTAAGACATG	Forward primer for confirmation of *acrB* knockout by PCR	Sigma
nudB_upstream_fw	GGCAGTCAACGAAGAGGCAGCGTG	Forward primer for confirmation of *nudB* knockout by PCR	Sigma
glyA_upstream_fw	GTTAGCTGAGTCAGGAGATGCGGATG	Forward primer for confirmation of *glyA* knockout by PCR	Sigma
surA_upstream_fw	GCGGTTAATTGAAATGGAAAAAGTATG	Forward primer for confirmation of *surA* knockout by PCR	Sigma
lpxM_upstream_forward	TGATTTTTGCCTTATCCGAAACTGGAAAAGCATG	Forward primer for confirmation of *lpxM* knockout by PCR	Sigma
kan_mid_rev	AATGGGCAGGTAGCCGGATCAAGC	Reverse primer for confirmation of knockouts via PCR	Sigma

h) **Composition of buffers and solutions**

- **1X TE**: Contains 10 mM of Tris-Cl of pH 8.0 and 1 mM EDTA of pH 8.0

- **3M sodium acetate**: Contains 8.2 g of sodium acetate dissolved in 100 mL of autoclaved Milli-Q filtered water.

- **0.1M $CaCl_2$**: Contains 1.1 g of $CaCl_2$ dissolved in 100 mL of autoclaved Milli-Q filtered water.

- **50X TAE:** Contains 242 g of tris-base, 57.1 mL of glacial acetic acid and 100 ml of 0.5 M EDTA (pH 8) dissolved in 1000 mL of deionised H_2O.

- **1M sodium citrate:** Contains 26 g of sodium citrate dissolved in 100 mL of autoclaved Milli-Q filtered water.

- **10% SDS:** Contains 10 g of SDS dissolved in 100 mL of autoclaved Milli-Q filtered water.

2.1 Methods

1. **Media and Culture Conditions:**

- **Preparation of Luria-Bertani Broth (LB)**: LB was prepared by adding 2.5 g of Luria Bertani Broth, Miller (HiMedia Cat. ref: GM1245-500G) in 100 mL of purified water, and autoclaving at 15 psi pressure for 20 mins at 121°C.

- **Preparation of Luria-Bertani Agar (LA)**: LA was prepared by adding 8 g of Luria Bertani Agar, Miller (HiMedia Cat. ref: GM151-500G) in 200 mL of purified and autoclaving at 15 psi pressure for 20 mins at 121°C.

- **Strain and Culture Conditions:** The strains employed in the study are listed in Table 8.

Table 7: List of bacterial strains used in the study.

Strain	Source
E. coli K-12 BW25113	Available in the laboratory
E. coli K-12 BW25113 *ΔlpxM*	Obtained from Keio Collection (Baba et al., 2006)
E. coli K-12 BW25113 *ΔrfaH*	Obtained from Keio Collection (Baba et al., 2006)
E. coli K-12 BW25113 *ΔrfaG*	Obtained from Keio Collection (Baba et al., 2006)
E. coli K-12 BW25113 *ΔkdsC*	Obtained from Keio Collection (Baba et al., 2006)
E. coli K-12 BW25113 *ΔacrB*	Obtained from Keio Collection (Baba et al., 2006)
E. coli K-12 BW25113 *ΔatpG*	Obtained from Keio Collection (Baba et al., 2006)
E. coli K-12 BW25113 *ΔtolA*	Obtained from Keio Collection (Baba et al., 2006)
E. coli K-12 BW25113 *ΔsurA*	Obtained from Keio Collection (Baba et al., 2006)
E. coli K-12 BW25113 *ΔglyA*	Obtained from Keio Collection (Baba et al., 2006)
E. coli K-12 BW25113 *ΔnudB*	Obtained from Keio Collection (Baba et al., 2006)
E. coli K-12 MG1655	Available in the laboratory
E. coli K-12 MG1655 *ΔrfaG*	Generated by P1 transduction, and confirmed with PCR
E. coli K-12 MG1655 *ΔacrB*	Generated by P1 transduction, and confirmed with PCR
E. coli K-12 MG1655 *ΔnudB*	Generated by P1 transduction, and confirmed with PCR

E. coli K-12 MG1655 *ΔglyA*	Generated by P1 transduction, and confirmed with PCR
E. coli K-12 MG1655 *ΔsurA*	Generated by P1 transduction, and confirmed with PCR
E. coli K-12 MG1655 *ΔlpxM*	Generated by P1 transduction, and confirmed with PCR
E. coli K-12 MG1655 1TR1	Vinchhi and Yelpure et al., 2023
E. coli K-12 MG1655 2TR1	Vinchhi and Yelpure et al., 2023
E. coli K-12 MG1655 3TR1	Vinchhi and Yelpure et al., 2023
E. coli K-12 MG1655 4TR1	Vinchhi and Yelpure et al., 2023
E. coli K-12 MG1655 1TR1 *ΔrfaG*	Generated by P1 transduction, and confirmed with PCR
E. coli K-12 MG1655 2TR1 *ΔrfaG*	Generated by P1 transduction, and confirmed with PCR
E. coli K-12 MG1655 3TR1 *ΔrfaG*	Generated by P1 transduction, and confirmed with PCR
E. coli K-12 MG1655 4TR1 *ΔrfaG*	Generated by P1 transduction, and confirmed with PCR
E. coli K-12 MG1655 1TR1 *ΔacrB*	Generated by P1 transduction, and confirmed with PCR
E. coli K-12 MG1655 2TR1 *ΔacrB*	Generated by P1 transduction, and confirmed with PCR
E. coli K-12 MG1655 3TR1 *ΔacrB*	Generated by P1 transduction, and confirmed with PCR
E. coli K-12 MG1655 4TR1 *ΔacrB*	Generated by P1 transduction, and confirmed with PCR
E. coli K-12 MG1655 1TR1 *ΔnudB*	Generated by P1 transduction, and confirmed with PCR
E. coli K-12 MG1655 2TR1 *ΔnudB*	Generated by P1 transduction, and confirmed with PCR
E. coli K-12 MG1655 3TR1 *ΔnudB*	Generated by P1 transduction, and confirmed with PCR
E. coli K-12 MG1655 4TR1 *ΔnudB*	Generated by P1 transduction, and confirmed with PCR

E. coli K-12 MG1655 1TR1 *ΔlpxM*	Generated by P1 transduction, and confirmed with PCR
E. coli K-12 MG1655 2TR1 *ΔlpxM*	Generated by P1 transduction, and confirmed with PCR
E. coli K-12 MG1655 3TR1 *ΔlpxM*	Generated by P1 transduction, and confirmed with PCR
E. coli K-12 MG1655 4TR1 *ΔlpxM*	Generated by P1 transduction, and confirmed with PCR
E. coli K-12 MG1655 1TR1 *ΔglyA*	Generated by P1 transduction, and confirmed with PCR
E. coli K-12 MG1655 2TR1 *ΔglyA*	Generated by P1 transduction, and confirmed with PCR
E. coli K-12 MG1655 3TR1 *ΔglyA*	Generated by P1 transduction, and confirmed with PCR
E. coli K-12 MG1655 4TR1 *ΔglyA*	Generated by P1 transduction, and confirmed with PCR

- **Culture conditions:** Bacteria were cultured in LB broth or grown as colonies on LA supplemented with antibiotics as needed. Broth cultures were grown at 37°C with shaking at 180 rpm, and plates were incubated at 37°C. Glycerol stocks were prepared by mixing sterile 50% glycerol and saturated cultures in a 1:1 ratio, and stored at -80°C.

2. Preliminary Screen

- **Preparation of 96 well plate**: Sterile 96 well plates were employed in the study. The peripheral wells were filled with 300µL of autoclaved Milli-Q filtered water, and all inner wells were filled with 150µL of LB, or 150µL of LB supplemented with 300 ng/mL trimethoprim.

- **Growth and measurement of growth**: The strains *E. coli* K-12 BW25113 and the knockouts from the Keio collection (Baba et al., 2006) were inoculated into 150µL of LB and 150µL of LB supplemented with 300 ng/mL trimethoprim using sterile tips, and were allowed to grow overnight at 37°C without shaking. Growth was measured by taking OD_{600} readings in the plate reader for all strains.

- **Classification of sensitivity:** The growth of knockouts from the Keio collection were compared to that of the wild type in the same growth conditions. Knockouts were identified as hypersensitive, neutral or resistant based on their deviation from the mean growth of the wild type at LB + 300 ng/mL trimethoprim. For example, knockouts that displayed a

growth 2 standard deviations away from the mean were considered to be hypersensitive to trimethoprim.

3. Serial Dilution Spot Assay

- **Bacterial culturing:** Primary cultures were prepared by inoculating 10 µL of the respective glycerol stock in 3 mL of LB, and growing them overnight at 37°C in shaking conditions.

- **Serial dilution and spotting:** Sterile MCTs were filled with 900µL of LB, and a 10-fold serial dilution of overnight cultures was performed by transferring 100µL of the primary culture into 900µL of LB to obtain a 10-fold diluted culture. This was repeated from the newly diluted culture to generate a 100 diluted culture, and so on, until cultures of 1000, 10^4, 10^5, and 10^6 fold dilutions were generated. 10µL of each of the primary culture and the diluted cultures were immediately spotted on LA alone, or LA supplemented with the required antibiotic concentration (Figure 6). Spots were allowed to dry, and the plates were incubated at 37°C without shaking for 15 hours.

- **Estimation of viable colonies:** Spotted plates were analysed after 15 hours of growth, and the number of viable colonies were determined by counting the spots that displayed growth between 3 and 30 colonies, and estimating the colony forming units/mL (CFUs/mL). The CFUs/mL were calculated for all spotted strains on LA alone, and on LA supplemented with the antibiotic.

$$\frac{CFU}{mL} = \frac{(Colony\ forming\ units) * (Dilution\ Factor) * 1000}{volume\ spotted}$$

Figure 6.

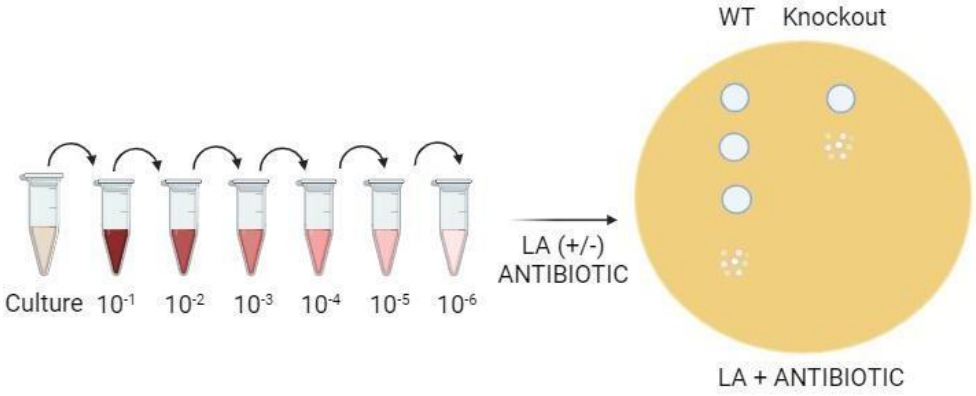

Figure 6: Schematic depicting serial dilution spot assay. Created with BioRender.com

\

4. **Generation of Knockouts**
   Knockouts were generated by following the protocol described by Thomason et al (Thomason et al., 2007).

- **Bacterial culturing:** Primary cultures were prepared by inoculating 10µL of the respective glycerol stock in 3 mL of LB, and growing them overnight at 37°C in shaking conditions.

- **P1 transduction:** All knockouts in the study in *E. coli* K-12 MG1655 were generated by P1 transduction (Figure 7).

  a. **Generation of donor lysate:** 1% of the primary culture of the donor strain, in this case, knockouts in *E. coli* K-12 BW25113 from the Keio collection, was inoculated in 5 mL LB containing 5mM $CaCl_2$, and grown for 1 hour at 37°C in shaking conditions. To this, 100 µL of P1 phage lysate carrying no selectable marker or different from the one in the Keio collection was added and incubated for 3 hours at 37°C in shaking conditions. 10-20 µL of $CHCl_3$ was added for lysis and vortexed. The lysate was then filtered through a 0.2 µm filter and stored at 4°C, for use as donor lysate.

  b. **Transduction into recipient strain:** 1% of the primary culture of the recipient stain was added to 3 mL of LB and grown for 3 hours at 37°C in shaking conditions. 1 mL of this culture was then supplemented with 5mM $CaCl_2$ and 100µL of donor lysate. As a control, 1 mL of the strain without the phage lysate (no phage), and 1 mL of LB with the phage lysate (no bacteria) were included. The cultures were then inoculated for 30 minutes at 37°C without shaking. To this, 0.1M sodium citrate was added and vortexed. The bacterial cells were pelleted down at 13,000rpm for 1 minute and resuspended in 1mL LB supplemented with 1M sodium citrate and incubated for 1.5 hours. The cultures were then centrifuged at 13,000rpm for 1 minute, 1 mL of the supernatant was discarded, and the pellet was resuspended in the remaining media. The suspension was then spread onto plates containing LA with 30 µg/mL of kanamycin, the selectable marker in the Keio collection.

- **Genomic DNA extraction**: Primary culture was prepared by inoculating 10 µL of the respective glycerol stock in 3 mL of LB, and growing it overnight at 37°C in shaking conditions. The culture was centrifuged at 13,000rpm for 1 minute, and the pellet was resuspended in 500 µL of 1X TE buffer. 50µL of SDS was then added, and the suspension was incubated for 1 hour at 37°C without shaking. To this, 5µl of proteinase K was added and incubated for 2 hours at 60°C without shaking on the thermomixer. 500 µL of phenol-chloroform-isoamyl alcohol (PCI) was then added, mixed thoroughly and then centrifuged at 13,000 rpm for 20 minutes. The aqueous phase was then transferred to fresh MCTs using a cut 200 µL tip, and 0.1 volumes of 3M sodium acetate and 2.5volumes of chilled 100% ethanol were added. The sample was centrifuged at 13,000 rpm for 1 minute, the supernatant was discarded and the cells were resuspended in 1mL of 70% ethanol. The sample was centrifuged at 13,000 rpm for 1 minute and the supernatant was discarded using a tip. The pellet was allowed to dry for 10-15 minutes, and then resuspended in 200 µL of autoclaved Milli-Q filtered water containing 2 mg/mL RNase A, and incubated at 37°C

without shaking overnight. The presence of genomic DNA was confirmed with gel electrophoresis and the extracted genomic DNA was stored at -20°C.

- **Knockout confirmation – PCRs:** Knockouts were confirmed with the help of PCRs by amplifying the region upstream of the gene till the 800th bp of the kanamycin cassette inserted in place of the gene to give rise to an 830 bp amplified product. Negative controls that lacked the knockout did not have an amplified 830 bp product. The reaction mixture was generated by adding 50% of either PrimeSTAR Max or ReadyMix Taq PCR, 35% of autoclaved Milli-Q filtered water, 2% of the required forward and reverse primer each, and 2% of the template DNA, obtained after genomic DNA extraction. The volume of the reaction mixture was maintained at 20 µL for all reactions. PCRs were run in the appropriate conditions based on the fidelity of the polymerase used in the reaction mixture.

- **Agarose gel electrophoresis:** A 1% agarose gel was prepared by boiling 1% agarose in 1x TAE buffer, supplementing with 1mg/mL ethidium bromide and allowing it to solidify. 6X loading dye was added to the samples in a 1:6 ratio, and was loaded into the wells along with the appropriate ladder. The gel was supplied with a voltage of 150 V, and was run in 1X TAE buffer until a sufficient resolution was achieved.

Figure 7.

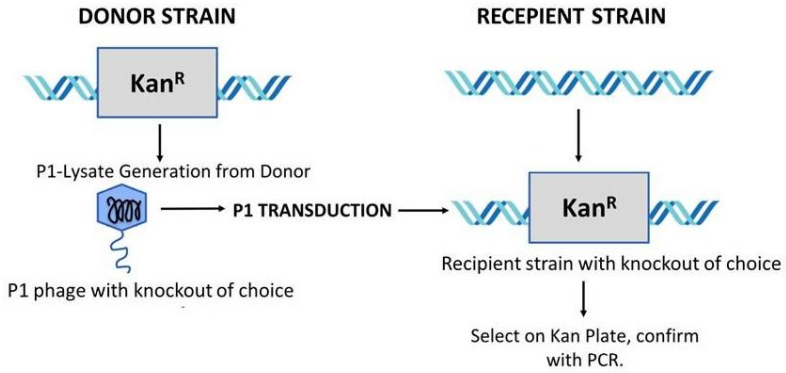

Figure 7: Schematic depicting P1 transduction. Created with BioRender.com

5. Broth Dilution Assay to Calculate IC50 Values

- **Preparation of 96-well plate:** Sterile 96 well plates were taken, and all peripheral wells were filled with autoclaved Milli-Q filtered water, and all inner wells were filled with 140 µL of LB. Wells B2, D2 and F2 were topped up with LB supplemented with trimethoprim to bring the final volume up to 290 µL of LB containing 1 mg/mL trimethoprim. A two-fold two-row serial dilution was performed by thoroughly mixing and then transferring 150 µL of LB from wells B2, D2 and F2 to wells B3, D3, and F3 respectively (Figure 8). This was continued up till B11, D11 and F11, and then continued from C2, E2 and G2 up till C10, E10 and G10, from which the excess LB was discarded. Wells C11, E11 and G11 were used as drug-free controls.

- **Growth and measurement of IC50 values:** Primary cultures were prepared by inoculating 10 µL of the respective glycerol stock in 3 mL of LB, and growing them for 6-8 hours at 37°C in shaking conditions. The cultures were diluted in a 1:10 ratio with LB in sterile MCTs, and 10 µL of the diluted cultures were immediately inoculated into the inner wells containing 140 µL of LB with a concentration gradient of trimethoprim. The 96-well plates were then covered with aluminum foil and incubated for 16 hours at 37°C without shaking. Growth was measured by taking OD_{600} readings of the plates in the plate reader after 16 hours of incubation. OD_{600} values for a single strain across the trimethoprim gradient were normalized to the strain's OD_{600} value in drug free condition, and were plotted against the log values of the antibiotic concentrations. A non-linear regression (4 parametric inhibition response curve) available in GraphPad version 9, was fitted to the data and IC50 values were determined.

Figure 8.

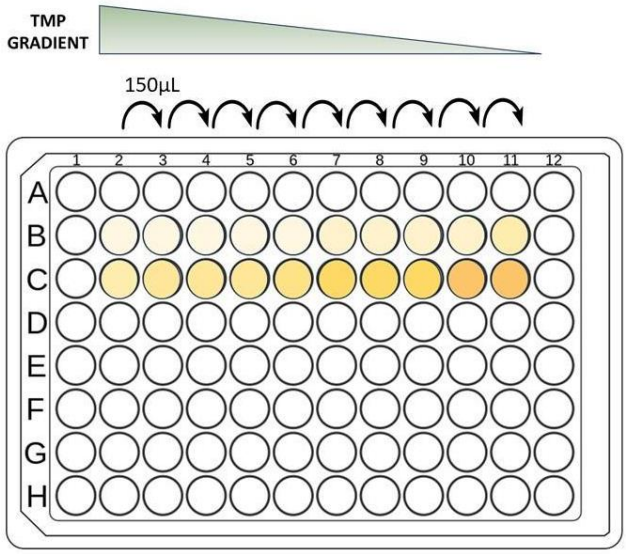

Figure 8: Schematic depicting broth dilution assay. Created with BioRender.com

6. Adaptive Laboratory Evolution of Antimicrobial Resistance

Knockouts were generated by following the protocol described by Vinchhi et al (Vinchhi et al., 2023).

1. **Bacterial culturing:** Primary cultures of the wild type and the knockouts were prepared by inoculating 10 µL of the respective glycerol stock in 3 mL of LB, and growing them overnight at 37°C in shaking conditions.

2. **Preparation of 96 well plate:** Adaptive laboratory evolution of the wild type and the knockouts were performed in 96 well plates. Sterile 96 well plates were taken, and all peripheral wells were filled with autoclaved Milli-Q filtered water. All wells in column 2 were filled with 150 µL of LB alone or LB supplemented with the appropriate concentration

of trimethoprim required for evolution (1 µg/mL for evolution at MIC, and 100 ng/mL for evolution at sub-MIC). This was repeated on day 2 for passage 2 in column 3 and so on until day 10. On day 11, a fresh sterile 96 well plate was taken, and the same process was repeated until day 20.

3. **Inoculation and evolution of resistance:** 1% of the overnight primary culture was inoculated into 150 µL of LB alone or LB supplemented with trimethoprim in wells B2, C2, D2, E2, F2 and G2 in column 2 in order to obtain independently evolving lineages. The plate was covered with aluminium foil and incubated for 24 hours at 37°C without shaking. Column 3 was then filled with the appropriate media conditions, and 1% of culture from column 2 was thoroughly mixed and passaged into the appropriate wells in column 3, making sure that the lineages remained separate (Figure 9). This was continued up to 20 passages (140 generations) or until the bacterial populations crashed, which was checked for after every 5th passage by checking for visible bacterial growth. Glycerol stocks of the independently evolving lineages were routinely made after every five passages, by adding 120 µL of the culture to 120 µL of 50% glycerol.

Figure 9.

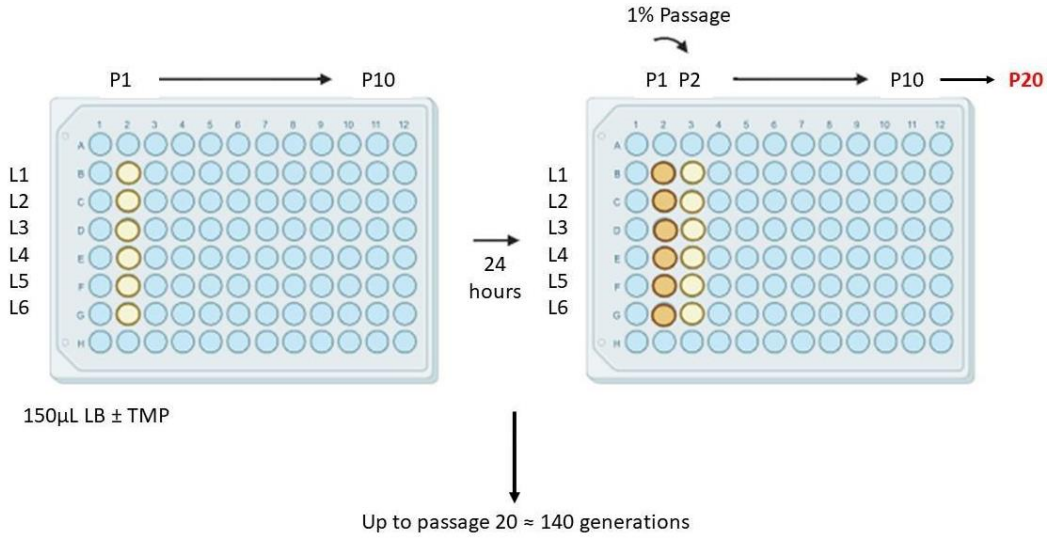

Figure 9: Schematic depicting adaptive laboratory evolution of antimicrobial resistance. Created with BioRender.com

7. **Checkerboard Assay**

Checkerboard assays were performed to check for synergy between trimethoprim and chlorpromazine (CPZ). The protocol followed was adapted from Orhan et al (Orhan et al., 2005).

- **Bacterial culturing:** A primary culture of *E. coli* K-12 MG1655 was prepared by inoculating 10µL of the glycerol stock in 3 mL of LB, and growing it for 6-8 hours at 37°C in shaking conditions.

- **Preparation of 96 well plate:** Sterile 96 well plates were taken, and all peripheral wells were filled with autoclaved Milli-Q filtered water. Two-fold serial dilutions of

trimethoprim were performed in sterile MCTs, with trimethoprim concentrations ranging from 6000 ng/mL to 25 ng/mL trimethoprim. 300 µL of LB containing 6000 ng/mL trimethoprim was added to well B2, and 150 µL of LB containing 6000 ng/mL was added to C2, D2, E2, F2, G2 of plate 1 and in B2, C2 and D2 of plate 2. Similarly, 300 µL of LB containing 3000 ng/mL trimethoprim was added to well B3, and 150µL of LB containing 3000 ng/mL was added to C3, D3, E3, F3, G3 of plate 1 and in B3, C3 and D3 of plate 2. This was continued to obtain a single-row two-fold serial dilution of trimethoprim until column 10, which contained 300 µL of LB containing 25 ng/mL trimethoprim in B10, and 150µL of LB containing 25 ng/mL in the remaining wells. Column 11 was maintained as a trimethoprim free control, and contained 300 µL of LB in well B11, and 150µL LB in the rest. All the inner wells of row B were then supplemented with 1000 µg/mL chlorpromazine, and a two-fold serial dilution was performed across the column by thoroughly mixing and transferring 15 0µL from wells B2-B11 to C2-C11. This was continued till row G of plate 1, and taken forward to rows B and C of plate 2, to get a single-column two-fold serial dilution of chlorpromazine. Row D (plate 2) was maintained as a chlorpromazine free control and contained only the gradient of trimethoprim. Well D11 was maintained as a drug free control as it contained neither of the drugs (Figure 10).

- **Inoculation and measurement of growth:** 1 µL of the primary culture of *E. coli* K-12 MG1655 was inoculated into all the inner wells of the 96 well plates. The 96-well plates were then covered with aluminum foil and incubated for 16 hours at 37°C without shaking. Growth was measured by taking OD_{600} readings of the plates in the plate reader after 16 hours of incubation.

- **Determination of synergy:** Synergy was determined by calculating the fractional inhibitory concentrations (FICs) at all the different combinations of concentrations of the two drugs. The FIC is determined by dividing the MICs of the drugs when in combination by the MIC of the drug when alone. If the value of the FIC is 0.05 and below, then the two drugs are said to interact synergistically, if the value lies between 0.5 and 4, then they are said to act additively, and if the value is greater than 4, then they are said to interact antagonistically (Scorzoni et al., 2016).

$$\sum \quad FIC = FIC_A + FIC_B = \frac{C_A}{MIC_A} + \frac{C_B}{MIC_B}$$

Figure 10.

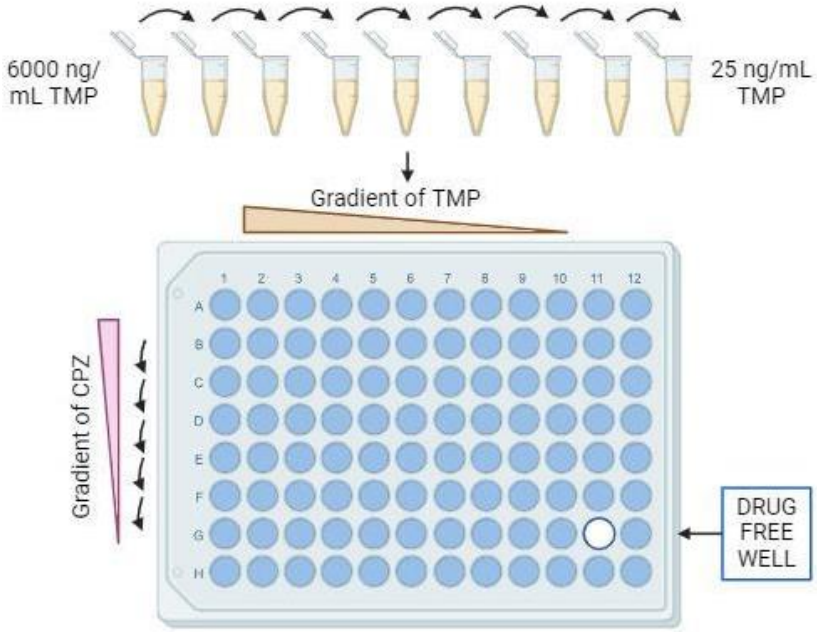

Figure 10: Schematic depicting concentration gradients in a checkerboard assay of TMP-CPZ. Created with BioRender.com

3. Results

a) Gene deletions that confer trimethoprim susceptibility are mostly related to defects in cell envelope structure and synthesis, followed by transport and information transfer.

In order to identify potential targets that could increase antibiotic susceptibility, a preliminary growth screen was performed on the Keio collection, a library of single gene deletions of all non-essential genes in the laboratory strain *Escherichia coli* K-12 BW25113 (Baba et al., 2006). In the screen, the growth of every strain in the collection was checked in LB-broth alone, or in LB-broth containing 300 ng/mL of trimethoprim (TMP). The gene knockouts that were compromised in the presence of the antibiotic compared to wild type were classified as trimethoprim hypersensitive. A total of 35 knockouts were more sensitive to trimethoprim than *E. coli* K-12 BW25113 wild type (WT). An analysis of the functional categories and gene ontologies of these knockouts revealed that 31% of the genes were involved in cell envelope structure and synthesis, 23% in metabolism and information transfer each, and 14% in transport [Figure 11].

Figure 11.

A.

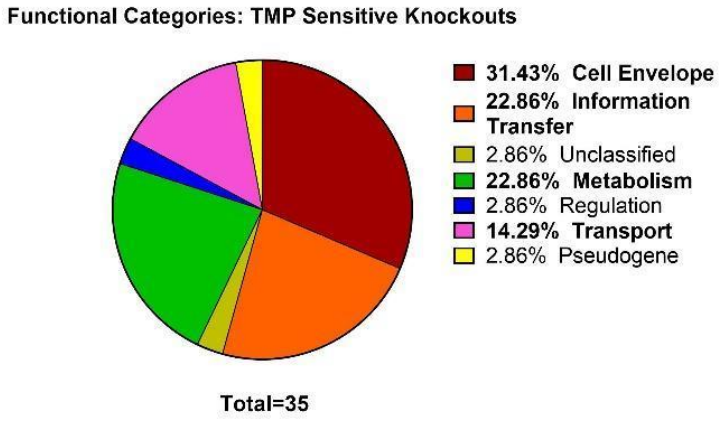

Figure 11: Functional categories of the 35 trimethoprim hypersensitive knockouts identified in the preliminary screen. Functional annotations obtained from Ecocyc.com

To check whether an enrichment in these categories in the screen was because of the inherent distribution of gene functions in *E. coli*, the distribution of functional categories for all annotated genes in *E. coli* was determined using Ecocyc (Keseler et al., 2021) as seen in Figure 12. Both the screen and the *E. coli* genome consisted of 15-20% of genes

involved in metabolism, indicating that loss of non-essential metabolic function was not enriched among trimethoprim hyper susceptible knockouts. However, this was not the case with transport, information transfer and cell wall related knockouts. The overall percentage of genes involved in these functions was significantly higher, suggesting that hampering these functions can lead to antibiotic hypersensitivity. This result was especially striking for cell wall knockouts since 30% of the hypersensitive knockouts in the screen were involved in cell envelope structure and synthesis, but only 4% of the *E. coli* genome were responsible for this function. These data indicated that defects in transport, information transfer and mainly cell wall synthesis increased trimethoprim susceptibility compared to *E. coli*.

Figure 12.

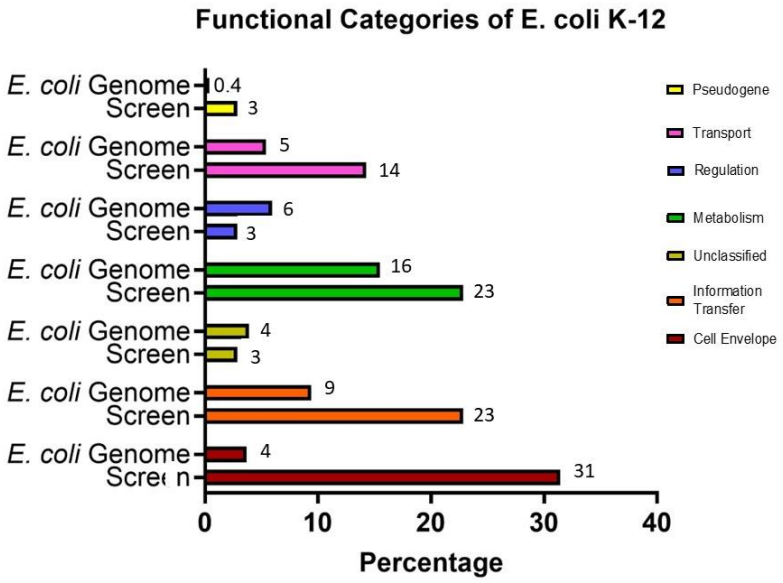

Figure 12: Percentage of functional categories in the preliminary screen versus annotated genes in E. coli K-12 MG1655. Functional annotations obtained from Ecocyc.com.

In order to validate the phenotype observed in the preliminary screen and eliminate possible false positives, 10 gene knockouts were selected and their ability to form colonies at different concentrations of trimethoprim, namely 100ng/mL, 300ng/mL and 900ng/mL, was determined (Table 9). Most knockouts that were involved in cell wall synthesis, transport and information transfer that either directly or indirectly accounted for different barriers of intrinsic resistance were taken forward for validation. Some knockouts that were more specific to the antibiotic and that did not modulate intrinsic resistance were also taken forward. For example, the knockout of *nudB,* which is involved in folate biosynthesis, was taken forward. The hypersensitivities of the knockouts were validated by comparing the number of viable colonies at a particular concentration of trimethoprim to the viable colonies produced by *E. coli* BW25113 wild type at the same concentration. As a control, *E. coli* MG1655 Δ*mgrB* was also spotted, since the loss of *mgrB* has been shown to confer trimethoprim tolerance in previously published literature from the lab (Patel and Matange., 2021). The *mgrB* knockout, unlike the ones from the screen, would be more resistant to

trimethoprim than the wild type. Strains that grew just as well as the wild type across all trimethoprim concentrations were considered to be false positives from the screen.

Table 8: List of mutants selected for validation of hypersensitivity and their definitions.

Mutants	Definition	GO Term	Citation
E. coli BW25113 Δ lpxM	Lipid A biosynthesis myristoyltransferase	Cell structure	Zhang et al., 2013.
E. coli BW25113 Δ rfaH	transcription antiterminator RfaH	Information transfer	Leeds and Welch., 1996.
E. coli BW25113 Δ rfaG	lipopolysaccharide glucosyltransferase I	Cell structure	Parker et al., 1992.
E. coli BW25113 Δ kdsC	3-deoxy-D-manno-octulosonate 8-phosphate phosphatase KdsC	Metabolism	Ray and Benedict., 1980.
E. coli BW25113 Δ acrB	multidrug efflux pump RND permease AcrB	Transport	Zgurskaya and Nikaido., 1999.
E. coli BW25113 Δ atpG	ATP synthase F1 complex subunit γ	Metabolism	Tang and Capaldi., 1996.
E. coli BW25113 Δ tolA	Tol-Pal system protein TolA	Cell structure	Levengood and Webster., 1999.
E. coli BW25113 Δ surA	chaperone SurA	Information transfer	Lazar and Kolter., 1996
E. coli BW25113 Δ glyA	Serine hydroxymethyltransferase	Metabolism	Stover and Schirch., 1990
E. coli BW25113 Δ nudB	dihydroneopterin triphosphate diphosphatase	Metabolism	Suzuki and Brown., 1974

The colony forming units/mL (CFU/mL) for each strain at different antibiotic concentrations were compared to that of the wild type, and hypersensitivity was validated. An example of this is shown in Figure 13. *E. coli* BW25113 Δ*acrB* grows just as well as the wild type strain in LA alone, but shows a 10,000-fold decrease when grown in LA +

100 ng/mL TMP, reiterating the results from the screen that the loss of *acrB* results in trimethoprim hyper susceptibility. Similarly, most knockouts from the screen continued to be more susceptible to trimethoprim than the wild type strain, barring *ΔkdsC*, as seen in Figure 14, with *ΔrfaG, ΔacrB, ΔsurA, ΔatpG* and *ΔlpxM* displaying the highest susceptibilities at 300ng/mL trimethoprim. The *kdsC* knockout was considered to be a false positive from the screen.

Figure 13.

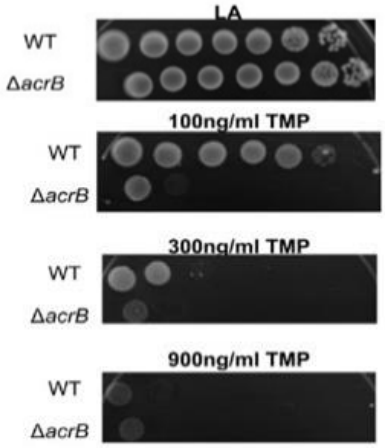

Figure 13: Validation of hypersensitivity conferred by loss of acrB at LA alone and LA supplemented with the indicated concentrations of trimethoprim. Spot images from one out of 3 independent replicates are shown.

Figure 14.

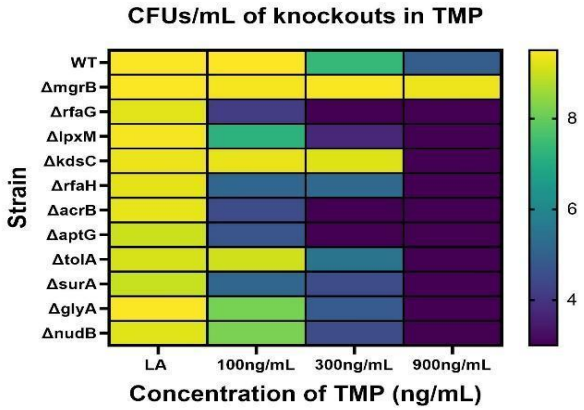

Figure 14: Log_{10} CFUs/mL of wild type and selected knockouts for validation in BW25113 at LA alone and LA supplemented with the indicated concentrations of trimethoprim. Average log_{10} CFU/mL from 3 independent replicates are shown, with scale representing the log(CFU/mL). Knockout of mgrB was used as a positive control

b) Deletion of *rfaG, acrB, lpxM* and *nudB* in *E. coli* MG1655 maintained hypersensitivity to trimethoprim.

Any prospective drug target with the ability to modulate antibiotic sensitivity should retain the same sensitive phenotype in all strains in which the target is present. Therefore, it was necessary to check whether the targets from the screen could confer trimethoprim sensitivity across different strains of *E. coli.* In order to check this, four of the most trimethoprim-susceptible knockouts from the screen that were also related to barriers of intrinsic resistance were transferred to *E. coli* K-12 MG1655. Two knockouts which were not involved in intrinsic resistance, but directly involved in folate biosynthesis were included as controls in the study. These 6 knockouts generated in *E. coli* MG1655 were as follows: *E. coli* K-12 MG1655 *ΔrfaG, E. coli* K-12 MG1655 *ΔacrB, E. coli* K-12 MG1655 *ΔlpxM, E. coli* K-12 MG1655 *ΔsurA, E. coli* K-12 MG1655 *ΔnudB,* and *E. coli* K-12 MG1655 *ΔglyA.*

The susceptibilities of these knockouts to trimethoprim were checked by serially diluting overnight cultures and spotting them onto solid media containing LA alone, LA+100 ng/mL TMP, LA+300 ng/mL TMP and LA+900 ng/mL TMP. Figure 15 represents a heat map of the $\log_{10}$ CFUs/mL of the different strains and the wild type strain at different concentrations of trimethoprim in both *E. coli* BW25113 and MG1655. While *ΔrfaG, ΔacrB, ΔlpxM* and *ΔnudB* retained their hypersensitive phenotype in *E. coli* MG1655, *ΔglyA* and *ΔsurA* did not; rather they grew slightly better than the wild type in the presence of the antibiotic. Similarly, when the susceptibilities of these strains were checked in liquid media by performing broth dilution assays, the IC50 values of *ΔrfaG, ΔacrB, ΔlpxM* and *ΔnudB* were significantly lower than that of the wild type, whereas that of *ΔglyA* and *ΔsurA* were not (Figure 16). Hence, the knockouts that were sensitive to trimethoprim in BW25113 continued to be sensitive in MG1655, barring *ΔglyA* and *ΔsurA*. The sensitivities displayed by *E. coli* BW25113 *ΔglyA* and *ΔsurA* could be attributed to background mutations that the strain may have acquired over time. Alternatively, there may be strain-specific differences between the functions of these genes.

Figure 15.

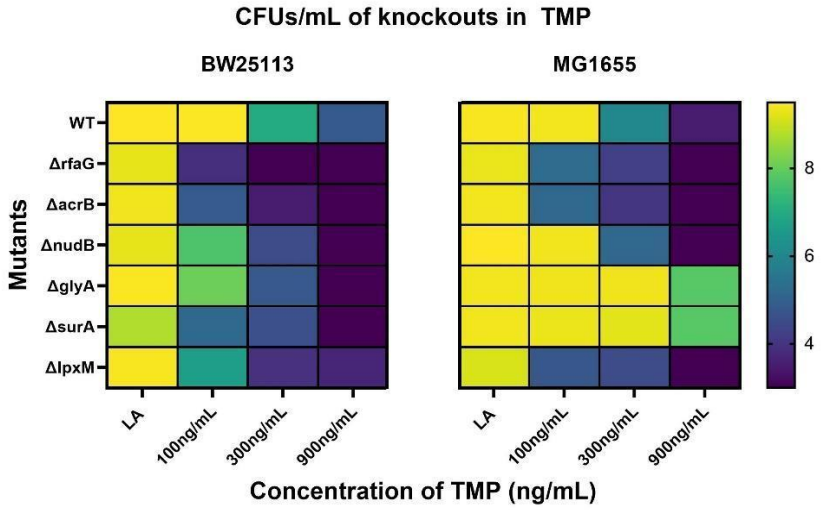

Figure 15: Log_{10} CFUs/mL of wild type and selected knockouts in BW25113 and MG1655 on LA alone or supplemented with indicated concentrations of trimethoprim. Average log_{10} CFU/mL from 3 independent replicates are shown, with scale representing the log(CFU/mL).

Figure 16.

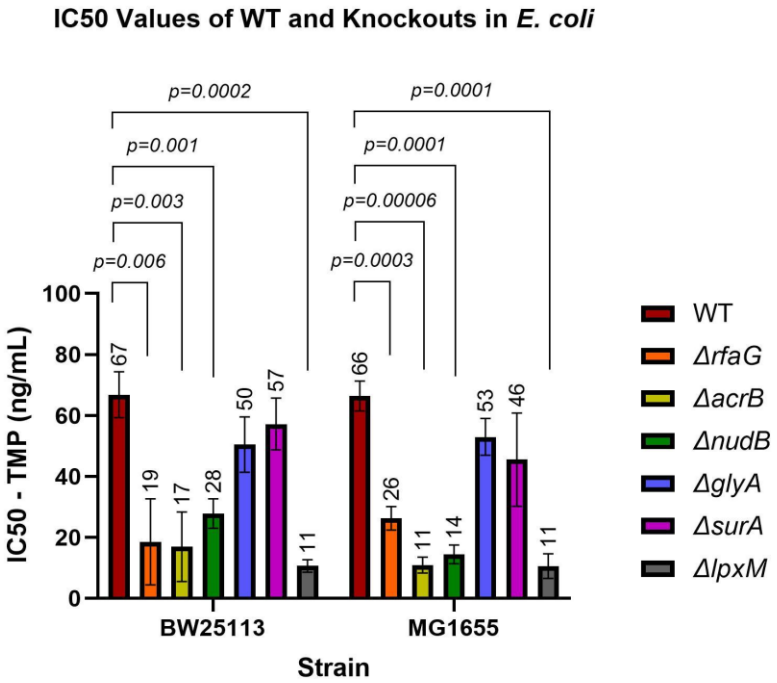

Figure 16: Trimethoprim IC50 values(ng/mL) of wild type and selected knockouts in BW25113 and MG1655 backgrounds. Average IC50 values and standard deviation from 3 independent replicates are shown. IC50 was determined by using Hill Function on Graphpad Version 9. P values were determined by unpaired students t-test on Graphpad Version 9.

c) Hypersensitive knockouts also resensitized trimethoprim-resistant strains to trimethoprim.

Having established that four knockouts could successfully sensitize different laboratory strains of *E. coli* to trimethoprim treatment, the next objective was to assess their potential to resensitize trimethoprim-resistant strains. Trimethoprim resistant strains from a previously performed laboratory evolution in the lab were used for this study (Vinchhi and Yelpure et al., 2023). These strains were generated by serially passaging wild type *E. coli* MG1655 in the presence of 100 ng/mL of trimethoprim (MIC/10 of the wild type) up to 210 generations. Four resistant strains were selected for the study, based on the resistance conferring mutation(s) they harboured [Figure 17].

Figure 17.

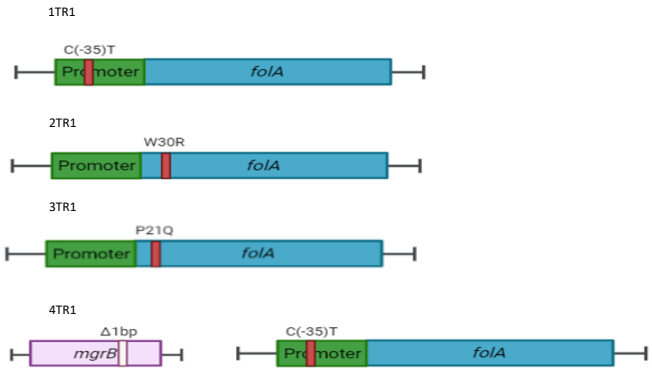

Figure 17: Schematic depicting trimethoprim resistant strains after 210 generations with their respective resistance conferring mutations, described in Vinchhi and Yelpure et al., 2023.

As depicted in Figure 14. A, strain 1TR1 contained a mutation in the promoter region of the *folA* gene, known to increase transcription of the gene, and therefore higher levels of DHFR. Strains 2TR1 and 3TR1 both contained mutations in the coding region of the *folA* gene, in the trimethoprim binding site, and the strain 4TR1 contained a promoter *folA* mutation along with a loss of function mutation in *mgrB,* both contributing to increased transcription of *folA.*

Following the generation of these knockouts in the resistant strains, broth dilution assays were performed to analyze the decrease in IC50 values compared to their resistant counterparts. Additionally, the IC50 values of the knockouts were compared to that of the wild type to understand whether the extent of resensitization and susceptibility was comparable to that of the wild type. Figure 18 represents the fold IC50 values in the knockouts and in the resistant strains with respect to the wild type.

Figure 18.

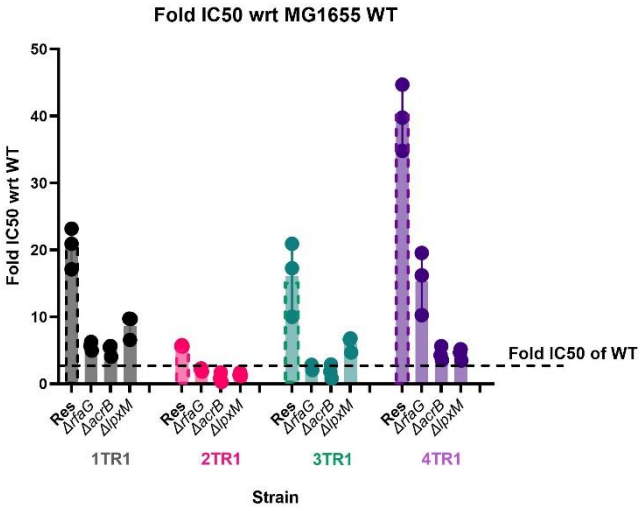

Figure 18: fold IC50 values of resistant strains and their knockouts wrt to the wild type. Fold IC50 of the wild type represented by the dotted line. Average IC50 values and standard deviation from 3 independent replicates are shown. IC50 was determined by using Hill Function on Graphpad Version 9.

As seen in Figure 18, all four knockouts successfully managed to resensitize trimethoprim-resistant strains to different extents irrespective of the resistance conferring mutation present. The *nudB* knockout notably exhibited the most substantial reduction in IC50 values in all strains, achieving IC50 values comparable or less than the wild type in most instances. Knockouts of *rfaG*, *acrB* and *lpxM* also successfully managed to resensitize the resistant strains to trimethoprim, achieving complete resensitization in strain 2TR1.

Thus, the knockouts that emerged from the screen related to some barrier of intrinsic resistance had the capability to reverse trimethoprim resistance, albeit to different extents, and achieve trimethoprim resensitization. As expected, the knockout involved in folate biosynthesis (*ΔnudB*) also possessed the same ability.

d) Knockouts that conferred trimethoprim hypersensitivity also conferred increased chloramphenicol susceptibility.

Due to the generic nature of intrinsic resistance mechanisms, inhibiting them was expected to enhance sensitivity to a broad range of antibiotics. To check this, the sensitivities of the above gene knockouts were checked against chloramphenicol (CMP), a protein synthesis inhibitor that binds to the 50S ribosomal subunit (Oong and Tadi., updated July 2023).

Cultures of individual gene knockouts were serially diluted and spotted on solid media containing LA alone, LA + 1.5 µg/mL CMP, LA + 3 µg/mL CMP and LA + 6 µg/mL CMP.

Figure 19 shows a heat map of the log_{10} CFUs/mL of the different strains and the wild type strain at different concentrations of chloramphenicol in *E. coli* BW25113.

Figure 19

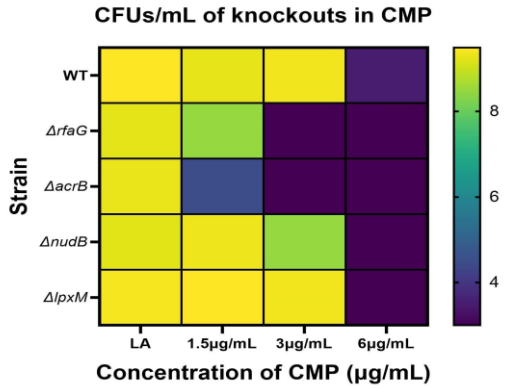

Figure 19: Log_{10} CFUs/mL of wild type and selected knockouts in BW25113 at LA alone and LA supplemented with the indicated concentrations of chloramphenicol. Average log_{10} CFU/mL from 3 independent replicates are shown, with scale representing the log (CFU/mL).

From Figure 19, it is evident that all the knockouts tested were also hypersensitive to chloramphenicol. This result was highly exacerbated for *ΔrfaG* and *ΔacrB* since they gave rise to far fewer viable colonies at concentrations that were both subinhibitory to the wild type, namely 1.5 μg/mL and 3 μg/mL CMP, and inhibitory to the wild type. While *ΔlpxM* grew just as well as the wild type at subinhibitory concentrations, at an inhibitory concentration of 6 μg/mL, it grew poorer than the wild type. Interestingly, *ΔnudB* also displayed a hypersensitive phenotype to chloramphenicol, though to a lesser extent than the other mutants. This observation may be explained by the close association between folate biosynthesis and methionine dependent translation via one carbon metabolism (Xu and Sinclair., 2015).

e) Trimethoprim hypersensitive knockouts regained resistance to differing extents when evolved under antibiotic pressure.

While the characterization of reversal of resistance is vital for the discovery of novel drug targets and resistance breaking agents, it is equally important to mitigate the risk of bacterial strains evolving resistance to these modulators and potentially compromising their efficacy. Therefore, it was essential to understand the evolutionary stability of the hypersensitive phenotype conferred by the knockouts. Six independent replicate lineages (L1-L6) of the wild type and the knockouts that modulate intrinsic resistance in *E. coli* MG1655 were evolved at the Minimum Inhibitory Concentration (MIC) of the wild type, and at a subinhibitory concentration (MIC/10) of the wild type.

When the strains were evolved at 1 µg/mL of trimethoprim (MIC of WT), three out of the six independently evolving lineages of the wild type displayed growth after 35 generations of growing at this concentration, whereas all lineages of the knockouts showed no growth and exhibited a population crash by the 14th generation (Figure 20). This observation indicated that at high concentrations of the antibiotic, all knockouts were compromised in their ability to recover from drug sensitivity.

It is well known that antibiotics, especially at sublethal concentrations can facilitate the development of antibiotic resistance (Gullberg et al., 2011). Therefore, all hypersensitive knockouts and the wild type were next evolved at 100 ng/mL of trimethoprim. This concentration represented MIC/10 of the wild type. Evolution of the different strains was carried out by serial passaging over 140 generations. All six lineages of the wild type and the knockouts displayed growth at 100 ng/mL even after 140 generations (Figure 20).

As controls six independent replicate lineages of the wild type and the knockouts were also evolved in the absence of the drug pressure, that is, in LB alone for 140 generations.

Figure 20.

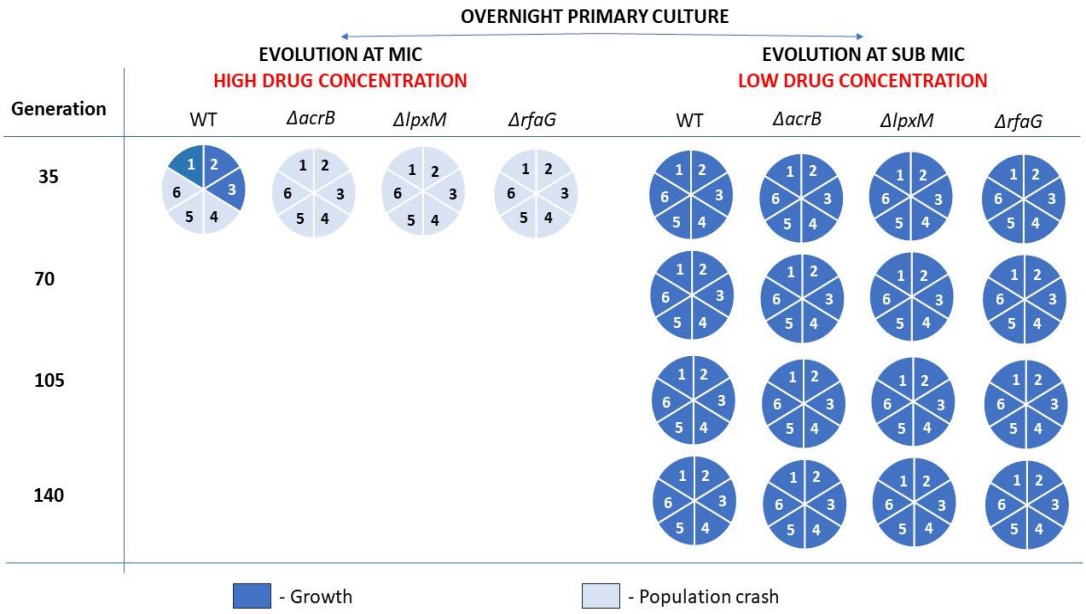

Figure 20: Schematic depicting evolution of trimethoprim resistance in six independently evolving lineages (L1-L6) of the wild type and the knockouts at the indicated concentrations of trimethoprim, across generations.

Gain of trimethoprim resistance after 140 generations was assessed by serially diluting overnight cultures of all lineages evolved in the absence of trimethoprim and in the presence of 100 ng/mL trimethoprim, and spotting them on solid media containing LA alone, or LA + 100 ng/mL TMP, LA + 300 ng/mL TMP and LA + 900 ng/mL TMP. Figure 21 represents heat maps of the CFUs/mL of the wild type and the knockouts after 140 generations of evolution compared to their respective ancestors. If the evolved lineages

showed better growth than their ancestor at the indicated concentrations of trimethoprim, then they were designated as trimethoprim resistant. If they grew better than the wild type ancestor at the highest concentration, which is near the MIC of the wild type, then they were characterized as having gained resistance past the breakpoint.

Figure 21.

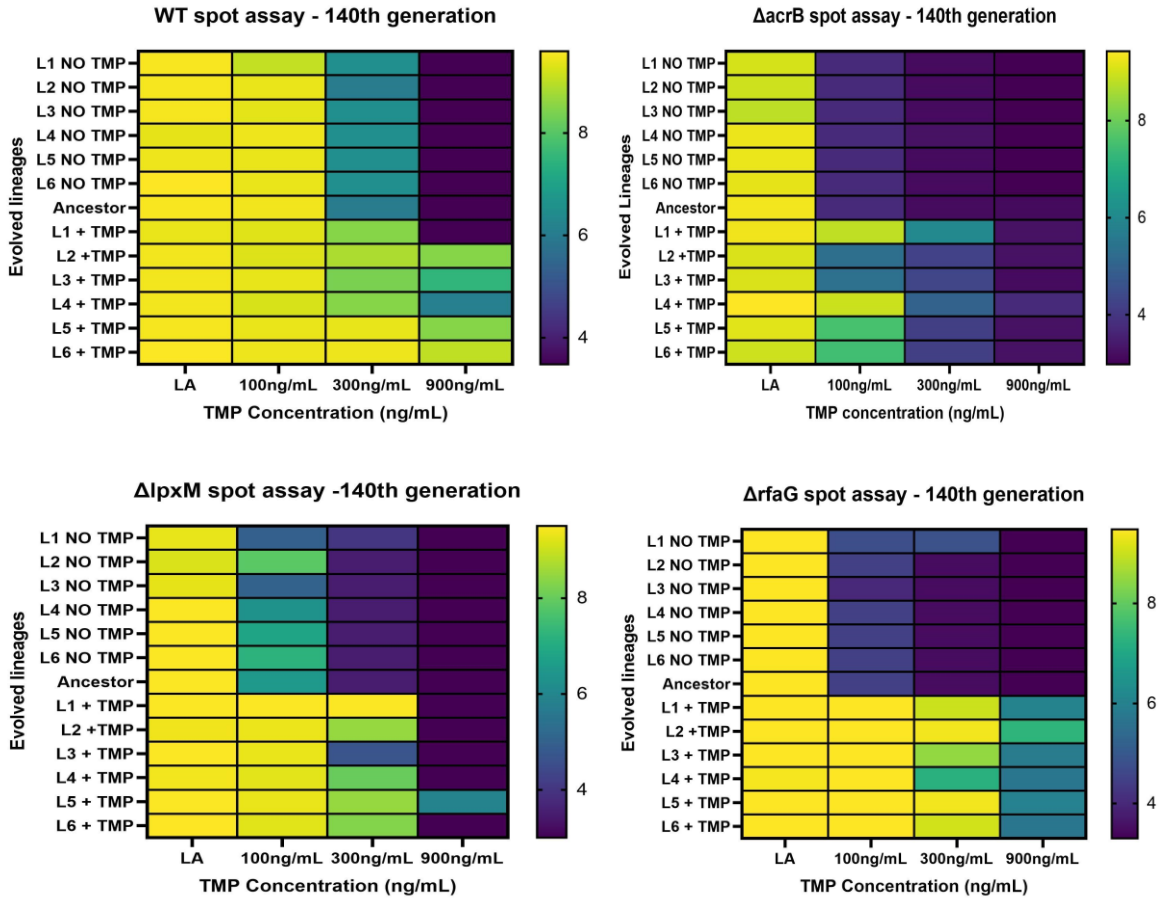

Figure 21: Log_{10} CFUs/mL of evolved strains after 140 generations/20 passages (P20) of the wild type and selected knockouts in LA only and LA supplemented with the indicated concentrations of trimethoprim. Average log_{10} CFU/mL from 2 independent replicates are shown, with scale representing the log(CFU/mL).

For wild type, the lineages evolved in LB alone displayed no change in their trimethoprim susceptibilities and behaved similar to their ancestor across all concentrations of trimethoprim. On the other hand, the lineages evolved in the presence of trimethoprim showed a marked gain in resistance, with five out of the six lineages crossing the breakpoint and giving rise to greater viable colonies at the MIC of the wild type. The same phenotype was observed in *ΔrfaG* lineages, with all six lineages evolving resistance compared to their ancestor and past the clinical breakpoint when passaged in the presence of the drug. Thus, while the *rfaG* knockout reversed resistance to trimethoprim, it could recover drug resistance reasonably rapidly under sub-MIC drug pressure. Interestingly, while the *ΔacrB*

and *ΔlpxM* lineages evolved resistance in the presence of the drug after 140 generations, the gain in resistance only conferred a benefit at subinhibitory concentrations of trimethoprim, but did not clear the wild type MIC breakpoint. These experiments showed that though there may be many possible ways to induce hypersensitivity to antibiotics, the evolutionary stability of hypersensitivity varied substantially between different mechanisms.

f) Trimethoprim resistance was conferred by mutations impacting folate synthesis across wild type and the knockouts, and elevated by mutations in outer membrane structure and synthesis.

Whole genome sequencing (WGS) was performed on all lineages of the wild type and the knockouts evolved in both the absence and the presence of trimethoprim to identify mutations that mediated trimethoprim adaptation in each genetic background. The results of the WGS were analyzed using Breseq, a computational pipeline that helps identify mutations relative to a reference sequence in haploid microbial genomes (Deatherage and Barrick., 2014). Figures 22-26 represent the mutations occurring in at least 20% of reads from the sequenced lineages evolved in the presence of trimethoprim.

In all six lineages of wild type evolved at 100 ng/mL trimethoprim, resistance was conferred either by genomic duplications (GDA) occurring in the *folA* region, possibly leading to increased DHFR production, or through mutations in the *folA* promoter and loss of function mutations in *mgrB,* both of which confer trimethoprim resistance in *E. coli* (Figure 22). These mutations may have been successful in enriching the trimethoprim resistant population and conferring resistance beyond the MIC of the wild type, as seen in Figure 21. Mutations were also observed in *fimE* and in *sspA* in lineages evolved with and without trimethoprim, indicating that these may represent media adaptations.

Figure 22.

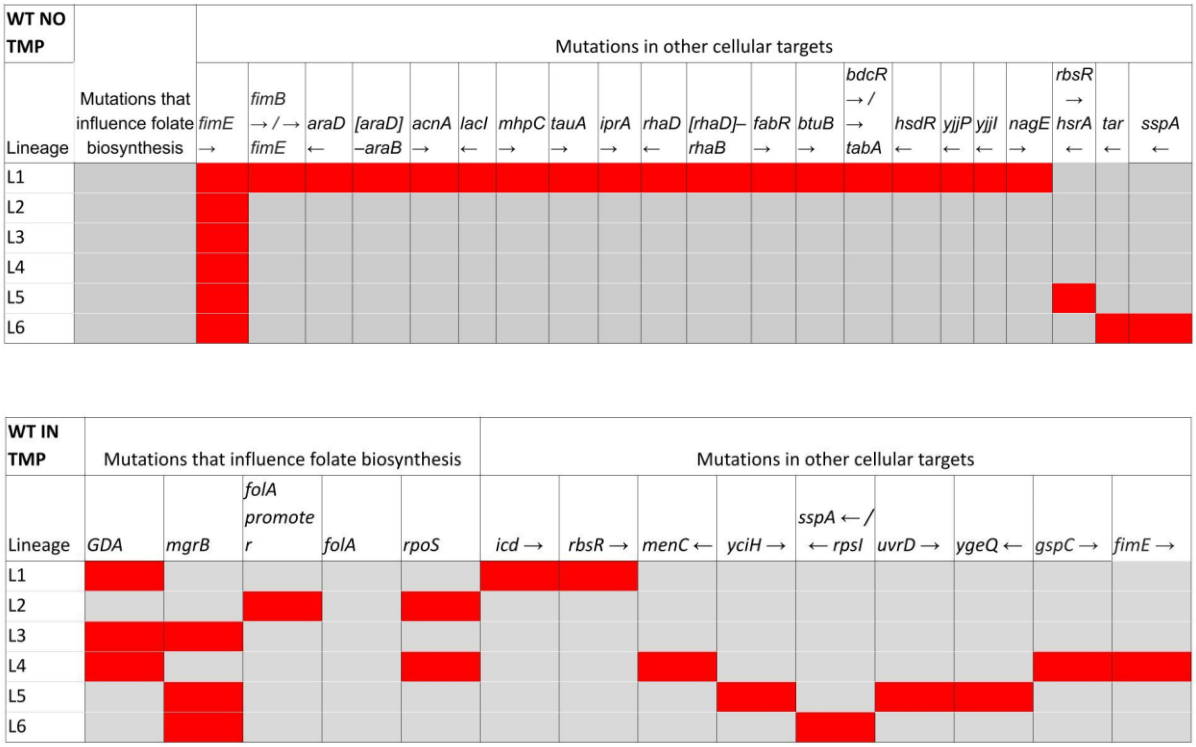

Figure 22: Genomic changes in the wild type (L1-6) evolved in LB alone (NO TMP) and LB + 100ng/mL trimethoprim (IN TMP) after 140 generations of evolution. Red indicates the presence of a mutation in the gene, and grey indicates the absence of a mutation in the gene.

Similarly, all lineages of *ΔacrB* (except L6) and *ΔlpxM* displayed mutations in the same set of genes as the wild type. Lineages of *ΔacrB* contained genomic duplications in the *folA* region, mutations in the promoter and coding region of *folA* and loss of function mutations in *mgrB*. Lineage L6 of the *acrB* knockout did not have any mutations in common with the other five lineages, whether it be in genes that influence folate biosynthesis or in other cellular targets. Rather, it had mutations in genes that are involved in sugar metabolism, porphyrin and fatty acid biosynthesis and cobalamin transport (Figure 23). Most mutations in L6 were also observed in wild type lineages evolved in LB alone, suggesting that these mutations may enable lineage 6 to compensate for the costs incurred during evolution. However, mutations in *ptsG*, *aceK* and *hemL* were exclusive to L6. While there is no evidence that these mutations affect folate synthesis or trimethoprim uptake/efflux and contribute to trimethoprim resistance, their combined effects may have led to a general

increase in resistance. Notably, L6 also showed very small increases in colony forming efficiency on trimethoprim possibly reflecting the mutations in this lineage.

Figure 23.

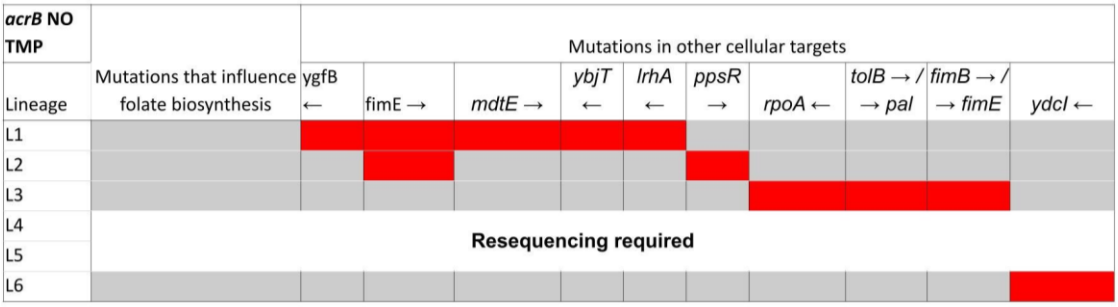

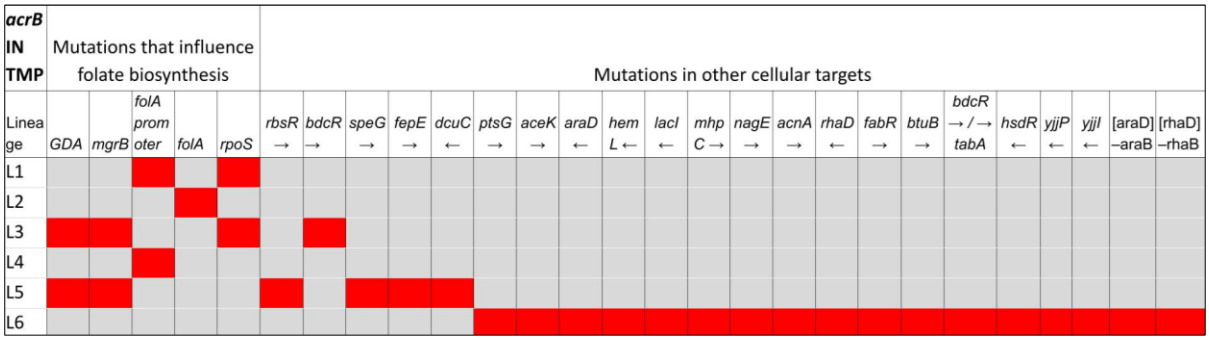

Figure 23: Genomic changes in ΔacrB (L1-6) evolved in LB alone (NO TMP) and LB + 100ng/mL trimethoprim (IN TMP) after 140 generations of evolution. Red indicates the presence of a mutation in the gene, and grey indicates the absence of a mutation in the gene.

Importantly, none of the lineages evolved in trimethoprim displayed mutations in genes involved in efflux activity or cell wall synthesis, indicating that there was no gain of a general mechanism of resistance, and the gain in resistance is specific to *folA*, or to a combined effect of multiple mutations. Since *ΔacrB* is a hypersensitive knockout, it should fix additional mutations compared to the ones in the wild type in order to gain resistance to the same level as the wild type. However, most lineages contained only a single mutation that conferred resistance to trimethoprim, which prevented them from gaining resistance beyond the breakpoint. In the lineages that contained both a genomic duplication of *folA* and mutations in *mgrB*, the resistance conferred was still below the breakpoint. These results reiterate the phenotype observed in Figure 21.

Interestingly, lineages passaged in LB alone displayed point mutations in *mdtE*, a membrane fusion protein belonging to a putative tripartite efflux pump (Saier et al., 2016),

and in the promoter of *pal*, which codes for the outer membrane component of the Tol-Pal system, and is important for maintaining lipopolysaccharide integrity (Mizuno, 1979). While these mutations may enable the lineages to compensate for the loss of *acrB*, such modifications in efflux and outer membrane integrity may promote the gain of broad-spectrum intrinsic resistance despite not encountering drug pressure. However, no such gain was observed against trimethoprim (Figure 21). Gain of resistance to other antibiotics is yet to be elucidated.

All lineages of *ΔlpxM* evolved with trimethoprim displayed genomic duplications in the *folA* region, and lineage 1 had a nonsense mutation in the 30th residue of *folM (*Figure 24), a dihydromonapterin reductase responsible for the synthesis of tetrahydromonapterin and tetrahydrofolate (to a lesser extent), which may contribute to resistance (Giladi et al., 2003, Pribat et al., 2010). Surprisingly, despite having perturbed cell wall synthesis, lineages evolved in the presence and absence of trimethoprim did not have mutations in genes involved in outer membrane synthesis. A 7 base pair insertion was observed in *prlF*, an antitoxin that is part of the PrlF-YhaV toxin-antitoxin complex (Fraikin and Goormaghtigh et al., 2020) in five out of the six lineages evolved in trimethoprim, with lineages 1, 5, 6 fixing this in more than 20% of their populations, but its contribution to resistance is yet to be elucidated. These results validate the phenotype observed in Fig 21. Similar to *ΔacrB*, *ΔlpxM* should fix additional mutations in order to gain resistance to the same level as the wild type. While genomic duplications could enrich resistance in the *lpxM* knockout compared to its ancestor, due to the lack of secondary mutations that confer resistance, the gain in resistance could not cross the breakpoint.

Figure 24.

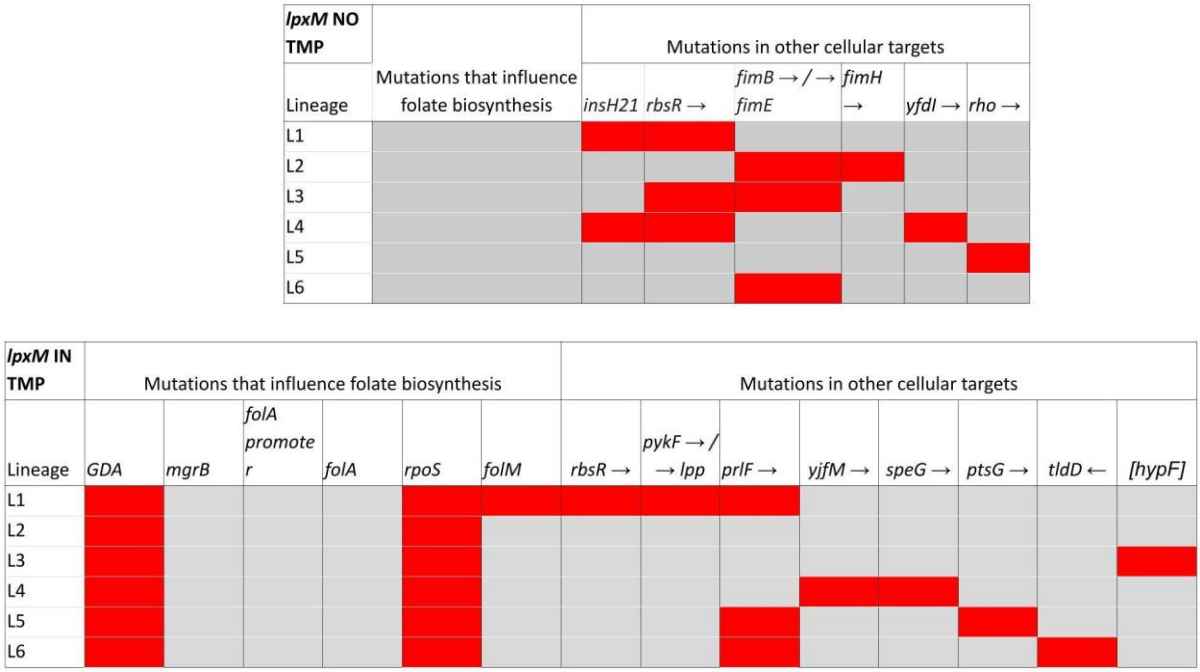

Figure 24: Genomic changes in ΔlpxM (L1-6) evolved in LB alone (NO TMP) and LB + 100ng/mL trimethoprim (IN TMP) after 140 generations of evolution. Red indicates the presence of a mutation in the gene, and grey indicates the absence of a mutation in the gene.

In the *rfaG* knockout, only three out of the six lineages evolved in trimethoprim (L1, L3 and L5) possessed loss of mutations in *mgrB,* and one (L3) had a point mutation in the *folD* promoter (Figure 25), which is involved in the synthesis of formyltetrahydrofolate, a precursor of tetrahydrofolate (D'Ari and Rabinowitz., 1991). Lineage 2 showed a genome duplication in the *folA* region. However, all six lineages displayed a clear increase in resistance well beyond the MIC of the wild type, despite L4 and L6 possessing no such mutations, as seen in Figure 16. B. While these lineages lacked mutations in genes that influence folate biosynthesis, they contained mutations in other cellular targets. Specifically, both lineages contained mutations in *dsbA,* specifically an insertion and a non-synonymous mutation. DsbA is a thiol disulphide oxidoreductase that is required for disulphide bond formation in some periplasmic proteins (Ito and Inaba., 2008). The deletion of DsbA has been shown to result in a PhoQ dependent increase in the expression of PhoP regulated genes (Lippa and Goulian., 2012). This could explain the gain in resistance observed in lineages 4 and 6.

Some lineages contained mutations in genes involved in outer membrane synthesis, which were also present in lineages evolved without trimethoprim (*lpxC, lptF, lptD* and *asmA* (Polissi and Sperandeo, 2014, Misra and Miao, 1995)). Not only could these mutations have compensated for the costs conferred by the *rfaG* knockout, but could also have conferred a general mechanism of broad-spectrum resistance by decreasing antibiotic uptake. While no such gain of trimethoprim resistance was observed in lineages passaged in LB alone (Figure 21), when combined with folate specific mutations, they may have the capability to elevate resistance beyond the breakpoint. The gain of resistance to other antibiotics in lineages containing these mutations is yet to be dissected.

Mutations were also consistently observed in *pitA,* a cation phosphate symporter in lineages evolved with trimethoprim (Willsky and Malamy., 1980). PitA has been shown to interact with MgtS, a PhoQP regulated small protein, to increase intracellular magnesium in Mg^{2+} limiting conditions, by preventing PitA mediated efflux of Mg^{2+} ions (Yin et al., 2019). Therefore, mutations in *pitA* may maintain low levels of Mg^{2+} in the cell, resulting in prolonged activation of the PhoQP system, leading to increased resistance. These mutations, coupled with mutations that directly influence folate synthesis, could enrich resistance beyond the MIC of the wild type, as observed in Figure 25.

Figure 25.

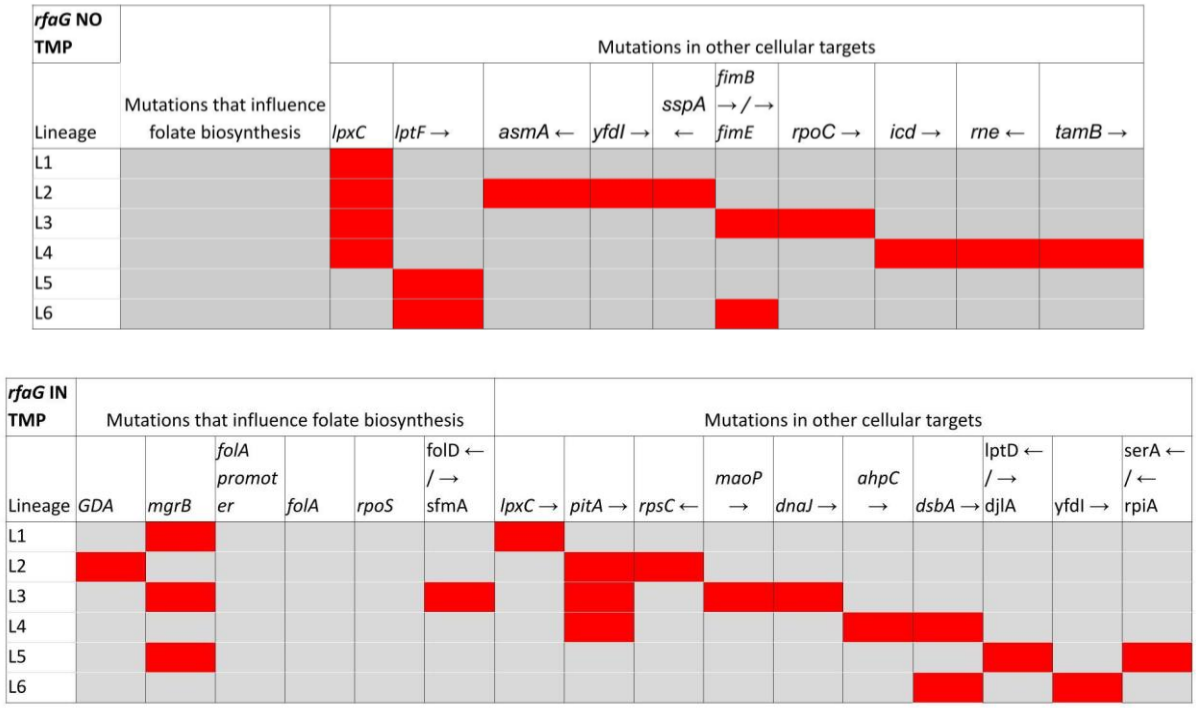

Figure 25: Genomic changes in ΔrfaG (L1-6) evolved in LB alone (NO TMP) and LB + 100ng/mL trimethoprim (IN TMP) after 140 generations of evolution. Red indicates the presence of a mutation in the gene, and grey indicates the absence of a mutation in the gene.

Therefore, as seen in result 3.5, all evolved strains of the wild type and the knockouts and displayed a gain in resistance compared to their ancestors, albeit to different extents, after 140 generations of evolution. This gain in resistance could be attributed to mutations that either directly or indirectly influence folate biosynthesis, or to mutations that affect cell wall structure and synthesis. Based on the combination of mutations present, the lineages can either achieve levels of resistance beyond the breakpoint of the wild type, as seen in *ΔrfaG*, or gain low levels of resistance, as seen in *ΔacrB* and *ΔlpxM* lineages. This result reiterates the potential of *acrB* and *lpxM* as excellent drug targets, since they do not fix multiple resistance conferring mutations despite evolving in drug pressure for 140 generations.

g) A chemical inhibitor of AcrB conferred trimethoprim hypersensitivity, but offered poor evolutionary stability of the hypersensitive phenotype under drug pressure.

Until now, our investigations have focused solely on studying hypersensitive phenotypes and scrutinising the evolutionary stability associated with these phenotypes in gene knockouts related to potential drug targets. However, it is crucial to recognize that gene knockouts do not authentically replicate the mechanism of adjuvants, since adjuvants work by competing with the substrate and chemically binding to and inhibiting the protein synthesised by these genes. Therefore, it was important to assess whether chemical inhibitors of the genes under examination could induce a comparable hypersensitive phenotype and check if this phenotype persists over the course of evolution.

Unfortunately, inhibitors of most of the genes under examination could not be procured due to their commercial unavailability. However, an inhibitor of AcrB, chlorpromazine, could be procured. Chlorpromazine is an antipsychotic that is used to treat and manage bipolar disorder, schizophrenia and acute psychosis (Mann and Marwaha., updated May 2023). Chlorpromazine has been shown to competitively bind at the hydrophobic trap within the distal binding pocket of AcrB, and inhibit AcrB mediated efflux by interfering with substrate binding (Grimsey et al., 2020). Therefore, chlorpromazine should potentially mimic the *acrB* knockout, and confer trimethoprim hyper susceptibility in the wild type strain when it is co-administered with trimethoprim.

In order to check for this, a combination therapy of chlorpromazine and trimethoprim were administered to *E. coli* MG1655 wild type strains via checkerboard assays. This combination was administered at varying concentrations of both the drugs, and inhibition was determined by comparing the growth in drug combination to the growth in single drug administration conditions and drug free conditions. Figure 18. A represents the inhibition of the wild type at varying concentrations of trimethoprim and chlorpromazine.

Figure 26.

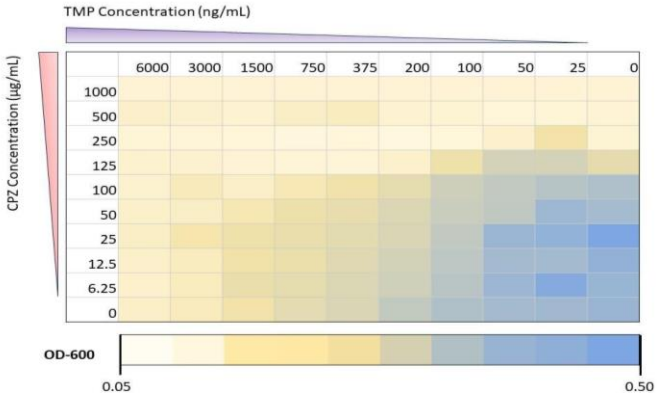

Figure 26: Checkerboard assay of trimethoprim-chlorpromazine (TMP-CPZ) combination therapy on E. coli MG1655 WT. OD_{600} values from one replicate out of three is shown.

The minimum inhibitory concentrations of trimethoprim and chlorpromazine were determined by analysing the individual concentrations of the drugs that led to 80% inhibition of MG1655 WT, and these were compared to the concentrations of the drugs in combination that achieved the same level of inhibition. For example, as seen in Figure 18. A, 80% inhibition of the wild type was observed at around 1500 ng/mL of trimethoprim and around 250µg/mL of chlorpromazine. However, a combination of 200 ng/mL trimethoprim and 125 µg/mL chlorpromazine (minimum combination concentrations) could achieve the same extent of inhibition of the wild type. Clearly, when administered with chlorpromazine, there was an eight-fold reduction in the concentration of trimethoprim required to inhibit the wild type.
The fractional inhibitory concentrations (FICs) were also determined at different concentrations in combination. The fractional inhibitory concentration is used to determine the extent of interaction between two drugs when administered in combination (Middleton et al., 1983).

When the FIC values were determined for the two drugs in combination, multiple combinations gave rise to an FIC value below 0.05, indicating that these compounds have the potential to interact synergistically, thereby increasing the susceptibility of the wild type to trimethoprim (Figure 27). Therefore, the addition of chlorpromazine along with trimethoprim mimicked the hypersensitive phenotype conferred by the *acrB* knockout and decreased the concentration of trimethoprim required to inhibit the wild type, compared to trimethoprim treatment alone.

Figure 27.

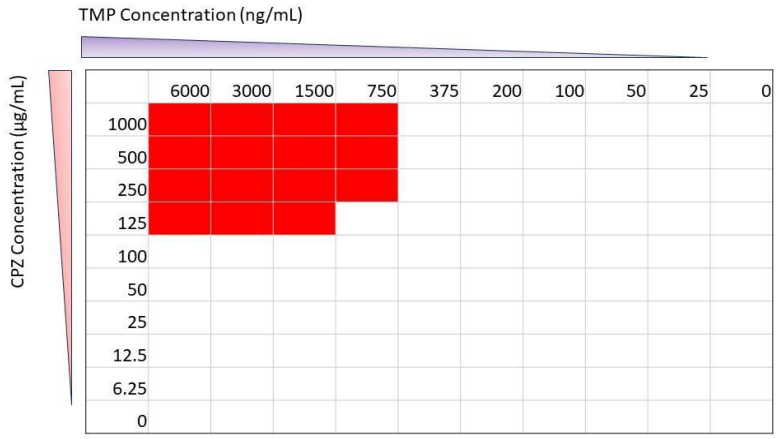

Figure 27: Synergism between CPZ and TMP against E. coli MG1655 WT cells using the fractional inhibitory concentration (FIC) index. Red indicates synergism between the two concentrations, with FIC values below 0.5. White indicates an additive effect, with FIC values between 0.5-4. Data from one replicate out of three are shown.

Similar to the investigation of the evolutionary stability of the hypersusceptible phenotype conferred by the genetic inhibition of *acrB*, it was also important to characterise the stability of this phenotype conferred by the chemical inhibitor of AcrB. Since the objective of the study was to understand the evolutionary stability of trimethoprim hyper-susceptibility, and not chlorpromazine susceptibility, a concentration of chlorpromazine that itself did not lead to any observable growth inhibition was selected for evolution. Six independent replicate lineages (L1-L6) of wild type *E. coli* MG1655 were evolved at 100 ng/mL (MIC/10) of trimethoprim, along with 50 µg/mL of chlorpromazine. The concentration of trimethoprim was selected as 100 ng/mL to ensure that both genetically and chemically inhibited *acrB* strains faced the same selection pressure. All six lineages of the wild type displayed growth at 100ng/mL TMP after 140 generations, indicating that like the *acrB* knockout, strains with a chemical inhibition of AcrB also have the potential to develop resistance at subinhibitory concentrations. Six independent replicate lineages of the wild type and the knockouts were also evolved only in 50 µg/mL of chlorpromazine for 140 generations, to identify what mutations help compensate for the inhibition of AcrB.

Figure 28 represents heat maps of the CFUs/mL of the lineages after 140 generations of evolution compared to their ancestor. Similar to the knockout lineages, if the evolved lineages showed better growth than the ancestor at the indicated concentrations of trimethoprim, then they were designated as trimethoprim resistant, and if they grew better than the ancestor at the MIC, then they were characterised as having gained resistance past the breakpoint.

Figure 28.

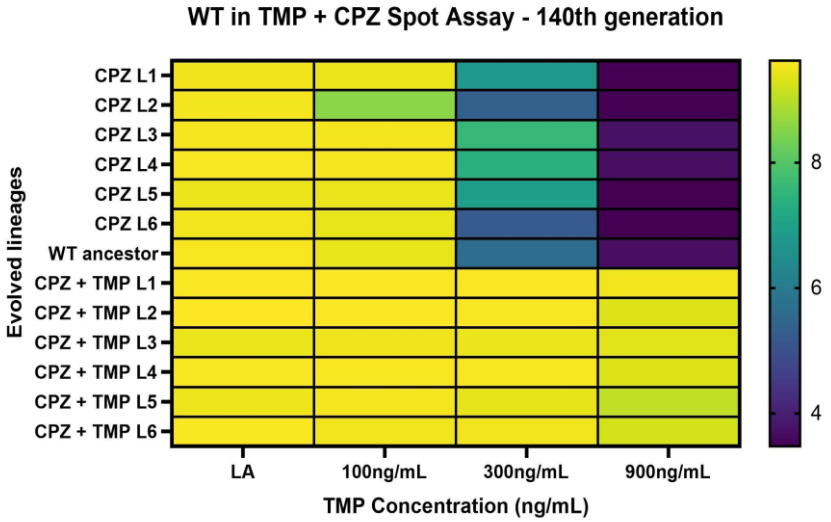

Figure 28: Log_{10} CFUs/mL of evolved strains after 140 generations/20 passages (P20) in LA only and LA supplemented with the indicated concentrations of trimethoprim. Average log_{10} CFU/mL from 2 independent replicates are shown, with scale representing the log(CFU/mL).

As seen in Figure 28, the lineages evolved in chlorpromazine alone grew similar or slightly better than the wild type ancestor at subinhibitory concentrations of trimethoprim. Near the MIC of the wild type, they showed no growth, and behaved similar to the ancestor. On the other hand, all 6 lineages evolved in the presence of chlorpromazine and trimethoprim showed a marked gain in resistance, with lineages outperforming the ancestor by a large margin at both subinhibitory concentrations and inhibitory concentrations of trimethoprim. While the gain in resistance in the evolved lineages of the *acrB* knockout only conferred a benefit at subinhibitory concentrations of trimethoprim, the chemical inhibition of AcrB led to a massive gain in resistance, indicating that while both mechanisms of inhibition can induce hypersensitivity to trimethoprim, the evolution of trimethoprim resistance between the two varies substantially. The mechanistic basis for these differences remains to be investigated.

4. Discussion

The rapid emergence of antibiotic resistance poses a significant risk to the efficacy of antibiotics and jeopardises the research efforts dedicated to antibiotic discovery and development. The overuse and misuse of antibiotics, along with a lack of new antibiotic development has exacerbated this crisis. Gram negative bacteria make up the most critical priority drug-resistant pathogens, with several of them displaying resistance to last resort antibiotics such as carbapenems and colistin. The mechanisms of intrinsic resistance are especially heightened in these bacteria due to the presence of the outer membrane. When coupled with multi-drug efflux, the effectiveness of antibiotics becomes drastically limited for these microbes (Impey and Hawkins et al., 2020). Studies have investigated the potential of compounds that work as membrane permeabilizers and efflux pump inhibitors to overcome intrinsic and acquired resistance. However, these studies focus on adjuvant pharmacodynamics and their ability to reverse resistance in drug-resistant bacteria. There exists a gap in the understanding of the evolutionary stabilities of the sensitivities conferred by these adjuvants. It is well established that resistance can develop to beta-lactamase inhibitors, and render the antibiotic-adjuvant combination therapy ineffective against pathogens (Oteo et al., 2008). Therefore, while it is important to identify targets that can reverse drug resistance, it is also vital to study their ability to evolve resistance when traces of the drugs are present.

In this study, we identified viable targets of intrinsic resistance that could modulate trimethoprim sensitivities in wild type and trimethoprim-resistant strains of *Escherichia coli* K-12, tested the stability of these phenotypes over the course of evolution, and tracked genomic changes that allowed for the evolution of resistance.

Although the sensitivities conferred by these knockouts have been characterised phenotypically, their mechanisms of sensitization are yet to be explained. Previous research has shown that antibiotic permeability can be increased by using compounds that perturb the cell wall. These perturbations can even allow the entry of gram-positive specific antibiotics into gram-negative bacteria, resulting in hypersensitivity to a completely different class of antibiotics (Wesseling and Martin., 2022). Since the inactivation of *rfaG* and *lpxM* would compromise the integrity of the outer membrane, the sensitivity and the reversal of resistance seen in these knockouts may be through greater antibiotic entry into the cell (Yethon et al., 2000, Douglass et al., 2021).

Similarly, while the mechanism of sensitivity in an *acrB* knockout is yet to be elucidated, it may do so by promoting the intracellular accumulation of the antibiotic. Several efflux pump inhibitors achieve antibiotic resensitization by competitively binding to efflux pumps and suppressing their activities, thereby leading to increased retention of the antibiotic within the cell (Zhang et al., 2024). Studies have also shown the prolonged retention and increased post-antibiotic effects of several antibiotics in *acrAB* mutants (Stubbings et al., 2005), suggesting that the *acrB* knockout allows for greater antibiotic retention, leading to hypersensitivity in wild type and resistant strains. Since these

mechanisms of antibiotic entry and retention are not specific to trimethoprim, this could explain why the knockouts were also sensitive to chloramphenicol. These results suggest that these knockouts have the potential to result in sensitivity to a broad spectrum of antibiotics. It is important to keep in mind that these mechanisms of sensitization may work only for antibiotics that exert their action within the cell, and not for antibiotics like polymyxins, which act on the outer membrane (Velkov et al., 2010).

A key finding from our study is that while both the genetic and chemical inhibition of intrinsic resistance result in hypersensitivity to trimethoprim, their evolutionary stabilities vastly differ. High concentrations well within the dosage of trimethoprim could not facilitate the evolution of resistance in the knockouts. On the other hand, evolution at subinhibitory concentrations of trimethoprim showed a gain in resistance in the knockouts compared to their ancestors. The *rfaG* knockout could facilitate a gain in resistance beyond the minimum inhibitory concentration of the wild type, but the *acrB* and *lpxM* knockouts only exhibited a gain in resistance at subinhibitory concentrations of trimethoprim.

Upon tracking the genomic changes in these knockouts, it was observed that *ΔacrB* and *ΔlpxM* lineages gained resistance only through mutations in genes that can modulate folate levels in the cell. No mutations in cell wall related genes or efflux related genes were observed. The observed mutations could only give rise to resistance to low concentrations of trimethoprim, implying that multiple mutations are required to elevate resistance beyond the breakpoint. However, the lack of occurrence of multiple mutations after 140 generations indicates that gaining additional mutations may come with a fitness cost in a *ΔacrB* and *ΔlpxM* background. This suggests that these strains cannot promote the evolution of elevated levels of resistance, and retain trimethoprim sensitivity at high concentrations of the antibiotic.

The *rfaG* knockout however, displayed mutations in genes that modulate folate levels, genes that affect outer membrane structure and synthesis, and in cation symporters. Specifically, these mutations occurred in combination, implying that there is no fitness cost to bearing these mutations together, and resulting in elevated levels of resistance well beyond the minimum inhibitory concentration of the wild type. While outer membrane modulations and cation symporters have not been directly implicated in trimethoprim resistance, the evidence in literature pointed out in result 7 alludes to their potential in heightening resistance.

The chemical inhibition of AcrB via chlorpromazine (CPZ) mimicked the *acrB* knockout and resulted in trimethoprim hyper susceptibility. Since CPZ competes with the substrate and binds to AcrB, the addition of CPZ along with trimethoprim probably resulted in the increased retention of trimethoprim in the cell. Curiously, when *E. coli* MG1655 wild type lineages were evolved at low concentrations of trimethoprim and CPZ for 140 generations, the lineages showed a sharp increase in resistance well beyond the minimum inhibitory concentration of the wild type, unlike their genetically inhibited counterpart. The ability to overcome drug sensitivity at high concentrations of trimethoprim is yet to be checked.

While the genomic changes of this gain of resistance are yet to be tracked, previous literature has shown that exposure to subinhibitory concentrations of chlorpromazine select for mutations in AcrAB-TolC regulatory genes in *E. coli*, such as *marR* and *acrR*

(Grimsey et al., 2020, MacGowan et al., 2023). These mutations lead to the upregulation and overexpression of AcrB-TolC expressed genes, and result in a gain of resistance to chlorpromazine. Higher activation of AcrAB-TolC has also been associated with resistance to multiple antibiotics (Piddock., 2006), implying that the evolution with chlorpromazine may not only promote the gain of resistance to chlorpromazine, but also to multiple classes of antibiotics that the bacteria have not been exposed to. Consequently, if bacteria are exposed to both chlorpromazine and an antibiotic, then they may evolve mutations that specifically inhibit the action of the antibiotic along with mutations to the efflux pump inhibitor, thereby leading to elevated levels of resistance against the exposed antibiotic and a general increase in resistance to multiple classes of antibiotics. In our study, all lineages evolved in the presence of trimethoprim and chlorpromazine displayed a massive gain in resistance, indicating that their populations may have fixed mutations in genes that influence folate levels along with mutations in regulatory genes of the AcrAB-TolC efflux pump.

The differences observed between genetic and chemical inhibition highlight the contrast in the mutational landscapes available to them. This is represented in Figure 29. In our study, the drug target was genetically inhibited by knocking out the entire gene and replacing it with a kanamycin cassette. In this case, there is no scope to regain activity in the inhibited target. Therefore, these strains can only evolve resistance to the antibiotic. This resonates with the mutations observed in *ΔacrB* lineages evolved in trimethoprim. However, since a chemical inhibitor of the drug-target binds to the target and confers sensitivity, strains can either evolve resistance against the chemical inhibitor by altering the binding site or overexpressing the target, or to the antibiotic, or unfavourably, to both. The chemical inhibition of AcrB led to elevated levels of trimethoprim resistance, implying that the lineages evolved resistance against the inhibitor, which also confers broad spectrum resistance, and evolved resistance to trimethoprim.

Figure 29.

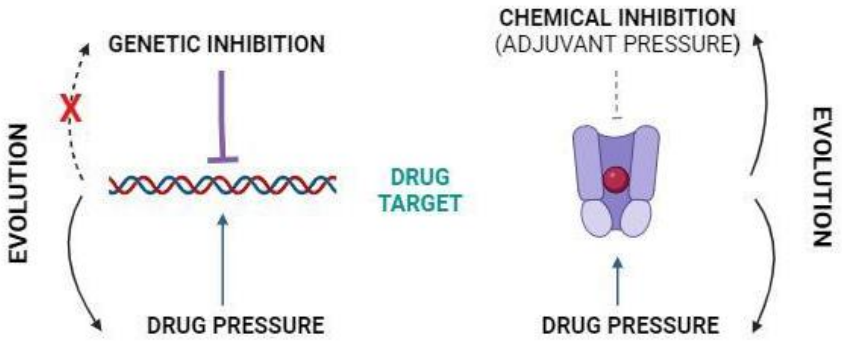

Figure 29: Schematic of available mutational landscapes for the evolution of resistance under drug pressure in genetically inhibited and chemically inhibited targets. Created with BioRender.com

While this assumption may be true for the chemical inhibition of AcrB with chlorpromazine, it may not apply to other inhibitors of AcrB, or to inhibitors of LpxM and

other potential targets. Therefore, it is important to test the gain of resistance upon exposure to these other chemicals in order to validate this assumption.

Nevertheless, these findings suggest that targeting intrinsic resistance may only be a viable strategy to combat antibiotic resistance as long as clinically relevant antibiotic-adjuvant dosages are maintained and administration policies are implemented. Inappropriate and unregulated use of the antibiotic-adjuvant may not only pose a risk of rapid evolution of resistance against both the antibiotic and the inhibitor, as observed in lineages evolved with CPZ-TMP, but also increase the possibility of developing resistance against multiple antibiotics due to the general nature and mechanism of the reversal of resistance by the adjuvant. Hence, while it is important to identify novel drug-targets to combat resistance, it is also equally vital to ensure that these antibiotic-inhibitor combinations are used responsibly. Public awareness campaigns, antibiotic stewardship programmes and education and training could help optimise antibiotic use and administration, and increase the efficacy of therapeutics.

5. Conclusion

In this study, we identified viable targets of intrinsic resistance that could modulate trimethoprim susceptibilities in *Escherichia coli.* We found that the genetic inhibition of intrinsic resistance could enhance trimethoprim susceptibility. Specifically, knockouts of *rfaG* and *lpxM,* which perturbed cell wall structure and synthesis, and of *acrB,* which disrupted drug efflux, conferred trimethoprim hypersensitivity across different strains of wild type *Escherichia coli* K-12, and could successfully resensitize trimethoprim resistant strains of *E. coli.* These knockouts could also sensitise *E. coli* to chloramphenicol, highlighting their potential to confer broad spectrum sensitivity. At high concentrations of the antibiotic, all knockouts were compromised in their ability to recover from drug sensitivity. At lower concentrations, while *ΔrfaG* recovered from drug sensitivity beyond the wild type breakpoint, *ΔacrB* and *ΔlpxM* continued to be sensitive to the MIC of wild type, highlighting their potential to serve as adjuvant targets. Importantly, a chemical inhibition of AcrB resulted in the evolution of resistance well beyond the breakpoint, when evolved at low drug concentrations, highlighting the different mechanisms that may be employed by genetically and chemically inhibited strains to overcome resistance, and reiterating the importance of drug dosage monitoring and responsible use of antibiotics.

6. Future Perspectives

For future perspectives, we propose several avenues for investigation. Firstly, we aim to expand our investigation beyond trimethoprim and chloramphenicol to identify knockout conferred hypersensitivity to a broad spectrum of antibiotics. Secondly, we seek to elucidate the impact of mutations observed post evolution on the acquisition of resistance within their respective knockout backgrounds. Thirdly, we intend to conduct comprehensive analyses of the mutational profiles in strains evolved under chlorpromazine alone or under chlorpromazine and trimethoprim, focussing on understanding the mechanisms of resistance gain. Additionally, we also plan to investigate the capacity of these mutations to confer broad spectrum resistance. Lastly, we aim to compare the magnitude of broad-spectrum resistance gain in genetically inhibited versus chemically inhibited drug targets.

7.References

1. Aboelenin, A. M., Hassan, R., & Abdelmegeed, E. S. (2021). The effect of EDTA in combination with some antibiotics against clinical isolates of gram negative bacteria in Mansoura, Egypt. Microbial Pathogenesis, 154, 104840.
2. Acosta-Gutierrez, S., Ferrara, L., Pathania, M., Masi, M., Wang, J., Bodrenko, I. et al. (2018) Getting drugs into Gram-negative bacteria: rational rules for permeation through general porins. ACS Infect. Dis. 4, 1487–1498
3. Ahmed, S., Sony, S.A., Chowdhury, M.B. *et al.* Retention of antibiotic activity against resistant bacteria harbouring aminoglycoside-*N*-acetyltransferase enzyme by adjuvants: a combination of in-silico and in-vitro study. *Sci Rep* 10, 19381 (2020).
4. Anoushiravani M, Falsafi T, Niknam V. Proton motive force-dependent efflux of tetracycline in clinical isolates of Helicobacter pylori. J Med Microbiol. 2009 Oct;58(Pt 10):1309-1313. doi: 10.1099/jmm.0.010876-0. Epub 2009 Jul 2. PMID: 19574414.
5. Antimicrobial Resistance Collaborators. Global burden of bacterial antimicrobial resistance in 2019: a systematic analysis. Lancet. 2022 Feb 12;399(10325):629-655. doi: 10.1016/S0140-6736(21)02724-0. Epub 2022 Jan 19. Erratum in: Lancet. 2022 Oct 1;400(10358):1102. PMID: 35065702; PMCID: PMC8841637.
6. Baba T, Ara T, Hasegawa M, Takai Y, Okumura Y, Baba M, Datsenko KA, Tomita M, Wanner BL, Mori H. Construction of Escherichia coli K-12 in-frame, single-gene knockout mutants: the Keio collection. Mol Syst Biol. 2006;2:2006.0008. doi: 10.1038/msb4100050. Epub 2006 Feb 21. PMID: 16738554; PMCID: PMC1681482.
7. Bhardwaj AK, Mohanty P. Bacterial efflux pumps involved in multidrug resistance and their inhibitors: rejuvinating the antimicrobial chemotherapy. Recent Pat Antiinfect Drug Discov. 2012 Apr;7(1):73-89. doi: 10.2174/157489112799829710. PMID: 22353004.
8. Birkle K, Renschler F, Angelov A, Wilharm G, Franz-Wachtel M, Maček B, Bohn E, Weber E, Müller J, Friedrich L, Schütz M. An Unprecedented Tolerance to Deletion of the Periplasmic Chaperones SurA, Skp, and DegP in the Nosocomial Pathogen Acinetobacter baumannii. J Bacteriol. 2022 Oct 18;204(10):e0005422. doi: 10.1128/jb.00054-22. Epub 2022 Sep 15. PMID: 36106853; PMCID: PMC9578438.
9. Bush K, Bradford PA. β-Lactams and β-Lactamase Inhibitors: An Overview. Cold Spring Harb Perspect Med. 2016 Aug 1;6(8):a025247. doi: 10.1101/cshperspect.a025247. PMID: 27329032; PMCID: PMC4968164.
10. Buynak JD. The discovery and development of modified penicillin- and cephalosporin-derived beta-lactamase inhibitors. Curr Med Chem. 2004 Jul;11(14):1951-64. doi: 10.2174/0929867043364847. PMID: 15279575.
11. Chancey ST, Zähner D, Stephens DS (2012) Acquired inducible antimicrobial resistance in Gram-positive bacteria. Future Microbiol 7: 959–978.
12. Chopra I, Roberts M. Tetracycline antibiotics: mode of action, applications, molecular biology, and epidemiology of bacterial resistance. Microbiol Mol Biol Rev. 2001

Jun;65(2):232-60 ; second page, table of contents. doi: 10.1128/MMBR.65.2.232-260.2001. PMID: 11381101; PMCID: PMC99026.
13. Chopra I. Molecular mechanisms involved in the transport of antibiotics into bacteria. Parasitology. 1988;96 Suppl:S25-44. doi: 10.1017/s0031182000085966. PMID: 3287290.
14. Cloeckaert A, Zygmunt MS, Doublet B. Editorial: Genetics of Acquired Antimicrobial Resistance in Animal and Zoonotic Pathogens. Front Microbiol. 2017 Dec 5;8:2428. doi: 10.3389/fmicb.2017.02428. PMID: 29259602; PMCID: PMC5723418.
15. Cox G, Wright GD. Intrinsic antibiotic resistance: mechanisms, origins, challenges and solutions. Int J Med Microbiol. 2013 Aug;303(6-7):287-92. doi: 10.1016/j.ijmm.2013.02.009. Epub 2013 Mar 13. PMID: 23499305.
16. D.J. Raines, T.J. Sanderson, E.J. Wilde, A.-K. Duhme-Klair, Siderophores, Reference Module in Chemistry, Molecular Sciences and Chemical Engineering, Elsevier, 2015, ISBN 9780124095472,
17. D'Ari L, Rabinowitz JC. Purification, characterization, cloning, and amino acid sequence of the bifunctional enzyme 5,10-methylenetetrahydrofolate dehydrogenase/5,10-methenyltetrahydrofolate cyclohydrolase from Escherichia coli. J Biol Chem. 1991 Dec 15;266(35):23953-8. PMID: 1748668.
18. de Kraker ME, Stewardson AJ, Harbarth S. Will 10 Million People Die a Year due to Antimicrobial Resistance by 2050? PLoS Med. 2016 Nov 29;13(11):e1002184. doi: 10.1371/journal.pmed.1002184. PMID: 27898664; PMCID: PMC5127510.
19. Deatherage, D.E., Barrick, J.E. (2014) Identification of mutations in laboratory-evolved microbes from next-generation sequencing data using breseq. Methods Mol. Biol. 1151: 165–188.
20. Delcour AH. Outer membrane permeability and antibiotic resistance. Biochim Biophys Acta. 2009 May;1794(5):808-16. doi: 10.1016/j.bbapap.2008.11.005. Epub 2008 Nov 27. PMID: 19100346; PMCID: PMC2696358.
21. Devon M Fitzgerald (2019) Bacterial Evolution: The road to resistance eLife 8:e52092
22. Ding F, Songkiatisak P, Cherukuri PK, Huang T, Xu XN. Size-Dependent Inhibitory Effects of Antibiotic Drug Nanocarriers against *Pseudomonas aeruginosa*. ACS Omega. 2018 Jan 31;3(1):1231-1243. doi: 10.1021/acsomega.7b01956. Epub 2018 Jan 30. PMID: 29399654; PMCID: PMC5793034.
23. Djoko KY, Achard MES, Phan MD, Lo AW, Miraula M, Prombhul S, Hancock SJ, Peters KM, Sidjabat HE, Harris PN, Mitić N, Walsh TR, Anderson GJ, Shafer WM, Paterson DL, Schenk G, McEwan AG, Schembri MA. Copper Ions and Coordination Complexes as Novel Carbapenem Adjuvants. Antimicrob Agents Chemother. 2018 Jan 25;62(2):e02280-17. doi: 10.1128/AAC.02280-17. PMID: 29133551; PMCID: PMC5786773.
24. Douglass MV, Cléon F, Trent MS. Cardiolipin aids in lipopolysaccharide transport to the gram-negative outer membrane. Proc Natl Acad Sci U S A. 2021 Apr 13;118(15):e2018329118. doi: 10.1073/pnas.2018329118. PMID: 33833055; PMCID: PMC8053950.
25. Durand-Réville TF, Guler S, Comita-Prevoir J, Chen B, Bifulco N, Huynh H, Lahiri S, Shapiro AB, McLeod SM, Carter NM, Moussa SH, Velez-Vega C, Olivier NB, McLaughlin R, Gao N, Thresher J, Palmer T, Andrews B, Giacobbe RA, Newman JV, Ehmann DE, de Jonge B, O'Donnell J, Mueller JP, Tommasi RA, Miller AA. ETX2514 is a broad-spectrum β-lactamase inhibitor for the treatment of drug-resistant Gram-negative

bacteria including Acinetobacter baumannii. Nat Microbiol. 2017 Jun 30;2:17104. doi: 10.1038/nmicrobiol.2017.104. PMID: 28665414.
26. Fontaine F, Héquet A, Voisin-Chiret AS, Bouillon A, Lesnard A, Cresteil T, Jolivalt C, Rault S. Boronic species as promising inhibitors of the Staphylococcus aureus NorA efflux pump: study of 6-substituted pyridine-3-boronic acid derivatives. Eur J Med Chem. 2015 May 5;95:185-98. doi: 10.1016/j.ejmech.2015.02.056. Epub 2015 Mar 2. PMID: 25817769.
27. Fraikin N, Goormaghtigh F, Van Melderen L. Type II Toxin-Antitoxin Systems: Evolution and Revolutions. J Bacteriol. 2020 Mar 11;202(7):e00763-19. doi: 10.1128/JB.00763-19. PMID: 31932311; PMCID: PMC7167474.
28. Ghai I, Ghai S. Understanding antibiotic resistance via outer membrane permeability. Infect Drug Resist. 2018 Apr 11;11:523-530. doi: 10.2147/IDR.S156995. PMID: 29695921; PMCID: PMC5903844.
29. Gholizadeh P, Köse Ş, Dao S, Ganbarov K, Tanomand A, Dal T, Aghazadeh M, Ghotaslou R, Ahangarzadeh Rezaee M, Yousefi B, Samadi Kafil H. How CRISPR-Cas System Could Be Used to Combat Antimicrobial Resistance. Infect Drug Resist. 2020 Apr 20;13:1111-1121. doi: 10.2147/IDR.S247271. PMID: 32368102; PMCID: PMC7182461.
30. Giladi M, Altman-Price N, Levin I, Levy L, Mevarech M. FolM, a new chromosomally encoded dihydrofolate reductase in Escherichia coli. J Bacteriol. 2003 Dec;185(23):7015-8. doi: 10.1128/JB.185.23.7015-7018.2003. PMID: 14617668; PMCID: PMC262705.
31. Grimsey EM, Fais C, Marshall RL, Ricci V, Ciusa ML, Stone JW, Ivens A, Malloci G, Ruggerone P, Vargiu AV, Piddock LJV. Chlorpromazine and Amitriptyline Are Substrates and Inhibitors of the AcrB Multidrug Efflux Pump. mBio. 2020 Jun 2;11(3):e00465-20. doi: 10.1128/mBio.00465-20. PMID: 32487753; PMCID: PMC7267879.
32. Gullberg E, Cao S, Berg OG, Ilbäck C, Sandegren L, Hughes D, Andersson DI. Selection of resistant bacteria at very low antibiotic concentrations. PLoS Pathog. 2011 Jul;7(7):e1002158. doi: 10.1371/journal.ppat.1002158. Epub 2011 Jul 21. PMID: 21811410; PMCID: PMC3141051.
33. Gupta S, Cohen KA, Winglee K, Maiga M, Diarra B, Bishai WR. Efflux inhibition with verapamil potentiates bedaquiline in Mycobacterium tuberculosis. Antimicrob Agents Chemother. 2014;58(1):574-6. doi: 10.1128/AAC.01462-13. Epub 2013 Oct 14. PMID: 24126586; PMCID: PMC3910722.
34. Halasohoris, S.A., Scarff, J.M., Pysz, L.M. et al. In vitro and in vivo activity of GT-1, a novel siderophore cephalosporin, and GT-055, a broad-spectrum β-lactamase inhibitor, against biothreat and ESKAPE pathogens. J Antibiot 74, 884–892 (2021).
35. Hall MJ, Middleton RF, Westmacott D. The fractional inhibitory concentration (FIC) index as a measure of synergy. J Antimicrob Chemother. 1983 May;11(5):427-33. doi: 10.1093/jac/11.5.427. PMID: 6874629.
36. Hinchliffe P, González MM, Mojica MF, González JM, Castillo V, Saiz C, Kosmopoulou M, Tooke CL, Llarrull LI, Mahler G, Bonomo RA, Vila AJ, Spencer J. Cross-class metallo-β-lactamase inhibition by bisthiazolidines reveals multiple binding modes. Proc Natl Acad Sci U S A. 2016 Jun 28;113(26):E3745-54. doi: 10.1073/pnas.1601368113. Epub 2016 Jun 14. PMID: 27303030; PMCID: PMC4932952.
37. Hinchliffe, P., Symmons, M. F., Hughes, C. & Koronakis, V. Structure and operation of bacterial tripartite pumps. *Annu. Rev. Microbiol.* **67**, 221–242 (2013).

38. Hutchings, M. I., Truman, A. W., & Wilkinson, B. (2019). Antibiotics: Past, present and future. *Current Opinion in Microbiology*, *51*, 72-80.
39. J. Schalk, Siderophore–antibiotic conjugates: exploiting iron uptake to deliver drugs into bacteria, Clin. Microbiol. Infect., 2018, 24, 801-802.
40. Impey RE, Hawkins DA, Sutton JM, Soares da Costa TP. Overcoming Intrinsic and Acquired Resistance Mechanisms Associated with the Cell Wall of Gram-Negative Bacteria. Antibiotics (Basel). 2020 Sep 19;9(9):623. doi: 10.3390/antibiotics9090623. PMID: 32961699; PMCID: PMC7558195.
41. Ito K, Inaba K. The disulfide bond formation (Dsb) system. Curr Opin Struct Biol. 2008 Aug;18(4):450-8. doi: 10.1016/j.sbi.2008.02.002. Epub 2008 Apr 11. PMID: 18406599.
42. Jamshidi S, Sutton JM, Rahman KM. Computational Study Reveals the Molecular Mechanism of the Interaction between the Efflux Inhibitor PAβN and the AdeB Transporter from *Acinetobacter baumannii*. ACS Omega. 2017 Jun 30;2(6):3002-3016. doi: 10.1021/acsomega.7b00131. Epub 2017 Jun 28. PMID: 30023681; PMCID: PMC6044690.
43. Kalan L, Wright GD. Antibiotic adjuvants: multicomponent anti-infective strategies. Expert Rev Mol Med. 2011 Feb 23;13:e5. doi: 10.1017/S1462399410001766. PMID: 21342612.
44. Keseler IM, Gama-Castro S, Mackie A, Billington R, Bonavides-Martínez C, Caspi R, Kothari A, Krummenacker M, Midford PE, Muñiz-Rascado L, Ong WK, Paley S, Santos-Zavaleta A, Subhraveti P, Tierrafría VH, Wolfe AJ, Collado-Vides J, Paulsen IT, Karp PD. The EcoCyc Database in 2021. Front Microbiol. 2021 Jul 28;12:711077. doi: 10.3389/fmicb.2021.711077. PMID: 34394059; PMCID: PMC8357350.
45. Khanna NR, Gerriets V. Beta Lactamase Inhibitors. [Updated 2022 Sep 26]. In: StatPearls [Internet]. Treasure Island (FL): StatPearls Publishing; 2022 Jan-. Available from: https://www.ncbi.nlm.nih.gov/books/NBK557592/
46. Krause KM, Serio AW, Kane TR, Connolly LE. Aminoglycosides: An Overview. Cold Spring Harb Perspect Med. 2016 Jun 1;6(6):a027029. doi: 10.1101/cshperspect.a027029. PMID: 27252397; PMCID: PMC4888811.
47. Krishnamoorthy, G., Leus, I.V., Weeks, J.W., Wolloscheck, D., Rybenkov, V.V. and Zgurskaya, H.I. (2017) Synergy between active efflux and outer membrane diffusion defines rules of antibiotic permeation into Gram-negative bacteria. mBio 8
48. Lazar SW, Kolter R. SurA assists the folding of Escherichia coli outer membrane proteins. J Bacteriol. 1996 Mar;178(6):1770-3. doi: 10.1128/jb.178.6.1770-1773.1996. PMID: 8626309; PMCID: PMC177866.
49. Leeds JA, Welch RA. RfaH enhances elongation of Escherichia coli hlyCABD mRNA. J Bacteriol. 1996 Apr;178(7):1850-7. doi: 10.1128/jb.178.7.1850-1857.1996. Erratum in: J Bacteriol 1996 Jul;178(13):3989. PMID: 8606157; PMCID: PMC177878.
50. Levengood SK, Webster RE. Nucleotide sequences of the tolA and tolB genes and localization of their products, components of a multistep translocation system in Escherichia coli. J Bacteriol. 1989 Dec;171(12):6600-9. doi: 10.1128/jb.171.12.6600-6609.1989. PMID: 2687247; PMCID: PMC210553.
51. Lippa AM, Goulian M. Perturbation of the oxidizing environment of the periplasm stimulates the PhoQ/PhoP system in Escherichia coli. J Bacteriol. 2012 Mar;194(6):1457-63. doi: 10.1128/JB.06055-11. Epub 2012 Jan 20. PMID: 22267510; PMCID: PMC3294871.

52. Liu Y, Lin Y, Wang Z, Hu N, Liu Q, Zhou W, Li X, Hu L, Guo J, Huang X, Zeng L. Molecular Mechanisms of Colistin Resistance in *Klebsiella pneumoniae* in a Tertiary Care Teaching Hospital. Front Cell Infect Microbiol. 2021 Oct 26;11:673503. doi: 10.3389/fcimb.2021.673503. PMID: 34765565; PMCID: PMC8576191.
53. Lomovskaya O, Warren MS, Lee A, Galazzo J, Fronko R, Lee M, Blais J, Cho D, Chamberland S, Renau T, Leger R, Hecker S, Watkins W, Hoshino K, Ishida H, Lee VJ. Identification and characterization of inhibitors of multidrug resistance efflux pumps in Pseudomonas aeruginosa: novel agents for combination therapy. Antimicrob Agents Chemother. 2001 Jan;45(1):105-16. doi: 10.1128/AAC.45.1.105-116.2001. PMID: 11120952; PMCID: PMC90247.
54. Louis B. Rice, Challenges in Identifying New Antimicrobial Agents Effective for Treating Infections with *Acinetobacter baumannii* and *Pseudomonas aeruginosa*, *Clinical Infectious Diseases*, Volume 43, Issue Supplement_2, September 2006, Pages S100–S105
55. MacGowan AP, Attwood MLG, Noel AR, Barber R, Aron Z, Opperman TJ, Grimsey E, Stone J, Ricci V, Piddock LJV. Exposure of Escherichia coli to antibiotic-efflux pump inhibitor combinations in a pharmacokinetic model: impact on bacterial clearance and drug resistance. J Antimicrob Chemother. 2023 Dec 1;78(12):2869-2877. doi: 10.1093/jac/dkad320. PMID: 37837411.
56. Mann SK, Marwaha R. Chlorpromazine. [Updated 2023 May 16]. In: StatPearls [Internet]. Treasure Island (FL): StatPearls Publishing; 2024 Jan-. Available from: https://www.ncbi.nlm.nih.gov/books/NBK553079/
57. Marquez B. Bacterial efflux systems and efflux pumps inhibitors. Biochimie. 2005 Dec;87(12):1137-47. doi: 10.1016/j.biochi.2005.04.012. PMID: 15951096.
58. Martinez JL. General principles of antibiotic resistance in bacteria. Drug Discov Today Technol. 2014 Mar;11:33-9. doi: 10.1016/j.ddtec.2014.02.001. PMID: 24847651.
59. Meletis G. Carbapenem resistance: overview of the problem and future perspectives. Ther Adv Infect Dis. 2016 Feb;3(1):15-21. doi: 10.1177/2049936115621709. PMID: 26862399; PMCID: PMC4735501.
60. Misra R, Miao Y. Molecular analysis of asmA, a locus identified as the suppressor of OmpF assembly mutants of Escherichia coli K-12. Mol Microbiol. 1995 May;16(4):779-88. doi: 10.1111/j.1365-2958.1995.tb02439.x. PMID: 7476172.
61. Mizuno T. A novel peptidoglycan-associated lipoprotein found in the cell envelope of Pseudomonas aeruginosa and Escherichia coli. J Biochem. 1979 Oct;86(4):991-1000. doi: 10.1093/oxfordjournals.jbchem.a132631. PMID: 115860.
62. Morones-Ramirez JR, Winkler JA, Spina CS, Collins JJ. Silver enhances antibiotic activity against gram-negative bacteria. Sci Transl Med. 2013 Jun 19;5(190):190ra81. doi: 10.1126/scitranslmed.3006276. PMID: 23785037; PMCID: PMC3771099
63. Morones-Ramirez, J. R., Winkler, J. A., Spina, C. S., & Collins, J. J. (2013). Silver Enhances Antibiotic Activity Against Gram-Negative Bacteria. Science Translational Medicine, 5(190), 190ra81–190ra81.
64. Mu S, Zhu Y, Wang Y, Qu S, Huang Y, Zheng L, Duan S, Yu B, Qin M, Xu FJ. Cationic Polysaccharide Conjugates as Antibiotic Adjuvants Resensitize Multidrug-Resistant Bacteria and Prevent Resistance. Adv Mater. 2022 Oct;34(41):e2204065. doi: 10.1002/adma.202204065. Epub 2022 Sep 12. PMID: 35962720.

65. National Centre for Biotechnology Information (2023). PubChem Compound Summary for CID 6333901, Auranofin. Retrieved March 15, 2023 from https://pubchem.ncbi.nlm.nih.gov/compound/Auranofin.
66. Nikaido H. Molecular basis of bacterial outer membrane permeability revisited. Microbiol Mol Biol Rev. 2003 Dec;67(4):593–656.
67. Nikaido H. Multidrug resistance in bacteria. Annu Rev Biochem. 2009;78:119-46. doi: 10.1146/annurev.biochem.78.082907.145923. PMID: 19231985; PMCID: PMC2839888.
68. Nikaido H. Structure and mechanism of RND-type multidrug efflux pumps. Adv Enzymol Relat Areas Mol Biol. 2011;77:1-60. doi: 10.1002/9780470920541.ch1. PMID: 21692366; PMCID: PMC3122131.
69. Nikaido, H. Molecular Basis of Bacterial Outer Membrane Permeability Revisited. Microbiol. Mol. Biol. Rev. **2003**, 67, 593–656.
70. Nordmann P, Cuzon G, Naas T. The real threat of Klebsiella pneumoniae carbapenemase-producing bacteria. Lancet Infect Dis. 2009 Apr;9(4):228–36.
71. Oong GC, Tadi P. Chloramphenicol. [Updated 2023 Jul 3]. In: StatPearls [Internet]. Treasure Island (FL): StatPearls Publishing; 2024 Jan-. Available from: https://www.ncbi.nlm.nih.gov/books/NBK555966/
72. Orhan G, Bayram A, Zer Y, Balci I. Synergy tests by E test and checkerboard methods of antimicrobial combinations against Brucella melitensis. J Clin Microbiol. 2005 Jan;43(1):140-3. doi: 10.1128/JCM.43.1.140-143.2005. PMID: 15634962; PMCID: PMC540140.
73. Osei Sekyere J, Amoako DG. Carbonyl Cyanide m-Chlorophenylhydrazine (CCCP) Reverses Resistance to Colistin, but Not to Carbapenems and Tigecycline in Multidrug-Resistant *Enterobacteriaceae*. Front Microbiol. 2017 Feb 14;8:228. doi: 10.3389/fmicb.2017.00228. PMID: 28261184; PMCID: PMC5306282.
74. Oteo J, Campos J, Lázaro E, Cuevas O, García-Cobos S, Pérez-Vázquez M, de Abajo FJ; Spanish Members of EARSS. Increased amoxicillin-clavulanic acid resistance in Escherichia coli blood isolates, Spain. Emerg Infect Dis. 2008 Aug;14(8):1259-62. doi: 10.3201/eid1408.071059. PMID: 18680650; PMCID: PMC2600377.
75. Papp-Wallace KM. The latest advances in β-lactam/β-lactamase inhibitor combinations for the treatment of Gram-negative bacterial infections. Expert Opin Pharmacother. 2019 Dec;20(17):2169-2184. doi: 10.1080/14656566.2019.1660772. Epub 2019 Sep 9. PMID: 31500471; PMCID: PMC6834881.
76. Parker CT, Kloser AW, Schnaitman CA, Stein MA, Gottesman S, Gibson BW. Role of the rfaG and rfaP genes in determining the lipopolysaccharide core structure and cell surface properties of Escherichia coli K-12. J Bacteriol. 1992 Apr;174(8):2525-38. doi: 10.1128/jb.174.8.2525-2538.1992. PMID: 1348243; PMCID: PMC205891.
77. Patel V, Matange N. Adaptation and compensation in a bacterial gene regulatory network evolving under antibiotic selection. Elife. 2021 Sep 30;10:e70931. doi: 10.7554/eLife.70931. PMID: 34591012; PMCID: PMC8483737.
78. Payne DJ, Miller LF, Findlay D, Anderson J, Marks L. Time for a change: addressing R&D and commercialization challenges for antibacterials. Philos Trans R Soc Lond B Biol Sci. 2015 Jun 5;370(1670):20140086. doi: 10.1098/rstb.2014.0086. PMID: 25918443; PMCID: PMC4424435.

79. Piddock LJ. Clinically relevant chromosomally encoded multidrug resistance efflux pumps in bacteria. Clin Microbiol Rev. 2006 Apr;19(2):382-402. doi: 10.1128/CMR.19.2.382-402.2006. PMID: 16614254; PMCID: PMC1471989.
80. Polissi A, Sperandeo P. The lipopolysaccharide export pathway in Escherichia coli: structure, organization and regulated assembly of the Lpt machinery. Mar Drugs. 2014 Feb 17;12(2):1023-42. doi: 10.3390/md12021023. PMID: 24549203; PMCID: PMC3944529.
81. Poole K. Efflux pumps as antimicrobial resistance mechanisms. Ann Med. 2007;39(3):162-76. doi: 10.1080/07853890701195262. PMID: 17457715.
82. Poole, K. Resistance to β-lactam antibiotics. *CMLS, Cell. Mol. Life Sci.* **61**, 2200–2223 (2004).
83. Pribat A, Blaby IK, Lara-Núñez A, Gregory JF 3rd, de Crécy-Lagard V, Hanson AD. FolX and FolM are essential for tetrahydromonapterin synthesis in Escherichia coli and Pseudomonas aeruginosa. J Bacteriol. 2010 Jan;192(2):475-82. doi: 10.1128/JB.01198-09. Epub 2009 Nov 6. PMID: 19897652; PMCID: PMC2805310.
84. Ramirez MS, Tolmasky ME. Aminoglycoside modifying enzymes. Drug Resist Updat. 2010 Dec;13(6):151-71. doi: 10.1016/j.drup.2010.08.003. Epub 2010 Sep 15. PMID: 20833577; PMCID: PMC2992599.
85. Ray PH, Benedict CD. Purification and characterization of specific 3-deoxy-D-manno-octulosonate 8-phosphate phosphatase from Escherichia coli B. J Bacteriol. 1980 Apr;142(1):60-8. doi: 10.1128/jb.142.1.60-68.1980. PMID: 6246070; PMCID: PMC293902.
86. Saier MH Jr, Reddy VS, Tsu BV, Ahmed MS, Li C, Moreno-Hagelsieb G. The Transporter Classification Database (TCDB): recent advances. Nucleic Acids Res. 2016 Jan 4;44(D1):D372-9. doi: 10.1093/nar/gkv1103. Epub 2015 Nov 5. PMID: 26546518; PMCID: PMC4702804.
87. Sanchez-Carbonel A, Mondragón B, López-Chegne N, Peña-Tuesta I, Huayan-Dávila G, Blitchtein D, Carrillo-Ng H, Silva-Caso W, Aguilar-Luis MA, Del Valle-Mendoza J. The effect of the efflux pump inhibitor Carbonyl Cyanide m-Chlorophenylhydrazone (CCCP) on the susceptibility to imipenem and cefepime in clinical strains of Acinetobacter baumannii. PLoS One. 2021 Dec 17;16(12):e0259915. doi: 10.1371/journal.pone.0259915. PMID: 34919563; PMCID: PMC8682880.
88. Sausville Edward, Principles of Clinical Pharmacology (Third Edition), Academic Press, 2012.
89. Silhavy TJ, Kahne D, Walker S. The bacterial cell envelope. Cold Spring Harb Perspect Biol. 2010 May;2(5):a000414. doi: 10.1101/cshperspect.a000414. Epub 2010 Apr 14. PMID: 20452953; PMCID: PMC2857177.
90. Stover P, Schirch V. Serine hydroxymethyltransferase catalyzes the hydrolysis of 5,10-methenyltetrahydrofolate to 5-formyltetrahydrofolate. J Biol Chem. 1990 Aug 25;265(24):14227-33. PMID: 2201683.
91. Stubbings W, Bostock J, Ingham E, Chopra I. Deletion of the multiple-drug efflux pump AcrAB in Escherichia coli prolongs the postantibiotic effect. Antimicrob Agents Chemother. 2005 Mar;49(3):1206-8. doi: 10.1128/AAC.49.3.1206-1208.2005. PMID: 15728929; PMCID: PMC549255.
92. Sun H, Zhang Q, Wang R, Wang H, Wong YT, Wang M, Hao Q, Yan A, Kao RY, Ho PL, Li H. Resensitizing carbapenem- and colistin-resistant bacteria to antibiotics using

auranofin. Nat Commun. 2020 Oct 16;11(1):5263. doi: 10.1038/s41467-020-18939-y. PMID: 33067430; PMCID: PMC7568570.
93. Sun J, Zhang H, Liu YH, Feng Y. Towards Understanding MCR-like Colistin Resistance. Trends Microbiol. 2018 Sep;26(9):794-808. doi: 10.1016/j.tim.2018.02.006. Epub 2018 Mar 7. PMID: 29525421.
94. Suzuki Y, Brown GM. The biosynthesis of folic acid. XII. Purification and properties of dihydroneopterin triphosphate pyrophosphohydrolase. J Biol Chem. 1974 Apr 25;249(8):2405-10. PMID: 4362677.
95. Tang C, Capaldi RA. Characterization of the interface between gamma and epsilon subunits of Escherichia coli F1-ATPase. J Biol Chem. 1996 Feb 9;271(6):3018-24. doi: 10.1074/jbc.271.6.3018. PMID: 8621695.
96. Tängdén T. Combination antibiotic therapy for multidrug-resistant Gram-negative bacteria. Ups J Med Sci. 2014 May;119(2):149-53. doi: 10.3109/03009734.2014.899279. Epub 2014 Mar 26. PMID: 24666223; PMCID: PMC4034552.
97. Thamilselvan G, Sarveswari HB, Vasudevan S, Stanley A, Shanmugam K, Vairaprakash P, Solomon AP. Development of an Antibiotic Resistance Breaker to Resensitize Drug-Resistant *Staphylococcus aureus*: *In Silico* and *In Vitro* Approach. Front Cell Infect Microbiol. 2021 Aug 16;11:700198. doi: 10.3389/fcimb.2021.700198. PMID: 34485178; PMCID: PMC8415528.
98. Thomason LC, Costantino N, Court DL. E. coli genome manipulation by P1 transduction. Curr Protoc Mol Biol. 2007 Jul;Chapter 1:1.17.1-1.17.8. doi: 10.1002/0471142727.mb0117s79. PMID: 18265391.
99. Vaara M. Agents that increase the permeability of the outer membrane. Microbiol Rev. 1992 Sep;56(3):395-411. doi: 10.1128/mr.56.3.395-411.1992. PMID: 1406489; PMCID: PMC372877.
100. Vedel G, Belaaouaj A, Gilly L, Labia R, Philippon A, Névot P, Paul G. Clinical isolates of Escherichia coli producing TRI beta-lactamases: novel TEM-enzymes conferring resistance to beta-lactamase inhibitors. J Antimicrob Chemother. 1992 Oct;30(4):449-62. doi: 10.1093/jac/30.4.449. PMID: 1490918.
101. Velkov T, Thompson PE, Nation RL, Li J. Structure--activity relationships of polymyxin antibiotics. J Med Chem. 2010 Mar 11;53(5):1898-916. doi: 10.1021/jm900999h. PMID: 19874036; PMCID: PMC2907661.
102. Vinchhi R, Yelpure C, Balachandran M, Matange N. Pervasive gene deregulation underlies adaptation and maladaptation in trimethoprim-resistant E. coli. mBio. 2023 Nov 30;14(6):e0211923. doi: 10.1128/mbio.02119-23. Epub ahead of print. PMID: 38032208; PMCID: PMC10746255.
103. Watson M, Liu JW, Ollis D. 2007. Directed evolution of trimethoprim resistance in Escherichia coli. The FEBS, Journal 274: 2661–2671.
104. Webber MA, Piddock LJ. The importance of efflux pumps in bacterial antibiotic resistance. J Antimicrob Chemother. 2003 Jan;51(1):9-11. doi: 10.1093/jac/dkg050. PMID: 12493781.
105. Wesseling CMJ, Martin NI. Synergy by Perturbing the Gram-Negative Outer Membrane: Opening the Door for Gram-Positive Specific Antibiotics. ACS Infect Dis. 2022 Sep 9;8(9):1731-1757. doi: 10.1021/acsinfecdis.2c00193. Epub 2022 Aug 10. PMID: 35946799; PMCID: PMC9469101.

106. White D.G., Maneewannakul K., Von Hofe E., Zillman M., Eisenberg W., Field A.K., Levy S.B. Inhibition of the multiple antibiotic resistance (mar) operon in Escherichia coli by antisense DNA analogs. *Antimicrob. Agents Chemother.* 1997;41:2699–2704. doi: 10.1128/AAC.41.12.2699
107. Willsky GR, Malamy MH. Characterization of two genetically separable inorganic phosphate transport systems in Escherichia coli. J Bacteriol. 1980 Oct;144(1):356-65. doi: 10.1128/jb.144.1.356-365.1980. PMID: 6998957; PMCID: PMC294655.
108. Willyard C. The drug-resistant bacteria that pose the greatest health threats. Nature. 2017 Feb 28;543(7643):15. doi: 10.1038/nature.2017.21550. PMID: 28252092.
109. Wise R, Hart T, Cars O, Streulens M, Helmuth R, Huovinen P, Sprenger M. Antimicrobial resistance. Is a major threat to public health. BMJ. 1998 Sep 5;317(7159):609-10. doi: 10.1136/bmj.317.7159.609. PMID: 9727981; PMCID: PMC1113826.
110. Wright GD. Antibiotic Adjuvants: Rescuing Antibiotics from Resistance. Trends Microbiol. 2016 Nov;24(11):862-871. doi: 10.1016/j.tim.2016.06.009. Epub 2016 Jul 15. Erratum in: Trends Microbiol. 2016 Nov;24(11):928. PMID: 27430191.
111. Xu J, Sinclair KD. One-carbon metabolism and epigenetic regulation of embryo development. Reprod Fertil Dev. 2015 May;27(4):667-76. doi: 10.1071/RD14377. PMID: 25710200.
112. Y. Yamano, In Vitro Activity of Cefiderocol Against a Broad Range of Clinically Important Gram-negative Bacteria, Clin. Infect. Dis., 2019, 69, S544-S551
113. Yethon JA, Vinogradov E, Perry MB, Whitfield C. Mutation of the lipopolysaccharide core glycosyltransferase encoded by waaG destabilizes the outer membrane of Escherichia coli by interfering with core phosphorylation. J Bacteriol. 2000 Oct;182(19):5620-3. doi: 10.1128/JB.182.19.5620-5623.2000. PMID: 10986272; PMCID: PMC111012.
114. Yin X, Wu Orr M, Wang H, Hobbs EC, Shabalina SA, Storz G. The small protein MgtS and small RNA MgrR modulate the PitA phosphate symporter to boost intracellular magnesium levels. Mol Microbiol. 2019 Jan;111(1):131-144. doi: 10.1111/mmi.14143. Epub 2018 Oct 21. PMID: 30276893; PMCID: PMC6351178.
115. Zeller V, Janoir C, Kitzis MD, Gutmann L, Moreau NJ. Active efflux as a mechanism of resistance to ciprofloxacin in Streptococcus pneumoniae. Antimicrob Agents Chemother. 1997 Sep;41(9):1973-8. doi: 10.1128/AAC.41.9.1973. PMID: 9303396; PMCID: PMC164047.
116. Zgurskaya HI, Nikaido H. Bypassing the periplasm: reconstitution of the AcrAB multidrug efflux pump of Escherichia coli. Proc Natl Acad Sci U S A. 1999 Jun 22;96(13):7190-5. doi: 10.1073/pnas.96.13.7190. PMID: 10377390; PMCID: PMC22048.
117. Zhanel GG, Lawrence CK, Adam H, Schweizer F, Zelenitsky S, Zhanel M, Lagacé-Wiens PRS, Walkty A, Denisuik A, Golden A, Gin AS, Hoban DJ, Lynch JP 3rd, Karlowsky JA. Imipenem-Relebactam and Meropenem-Vaborbactam: Two Novel Carbapenem-β-Lactamase Inhibitor Combinations. Drugs. 2018 Jan;78(1):65-98. doi: 10.1007/s40265-017-0851-9. Erratum in: Drugs. 2018 May 10;: PMID: 29230684.
118. Zhang G, Meredith TC, Kahne D. On the essentiality of lipopolysaccharide to Gram-negative bacteria. Curr Opin Microbiol. 2013 Dec;16(6):779-85. doi: 10.1016/j.mib.2013.09.007. Epub 2013 Oct 19. PMID: 24148302; PMCID: PMC3974409.

119. Zhang L, Tian X, Sun L, Mi K, Wang R, Gong F, Huang L. Bacterial Efflux Pump Inhibitors Reduce Antibiotic Resistance. Pharmaceutics. 2024 Jan 25;16(2):170. doi: 10.3390/pharmaceutics16020170. PMID: 38399231; PMCID: PMC10892612.
120. Zhang Y, Shi L, Lv L, Zhang Y, Chen H. Identification of a novel adjuvant loperamide that enhances the antibacterial activity of colistin against MCR-1-positive pathogens in vitro/vivo. Lett Appl Microbiol. 2023 Feb 16;76(2):ovad025. doi: 10.1093/lambio/ovad025. PMID: 36787890.